

University of Windsor

## Scholarship at UWindor

---

Electronic Theses and Dissertations

Theses, Dissertations, and Major Papers

---

Fall 2021

# Underwater Source Localization based on Modal Propagation and Acoustic Signal Processing

Luca Saeid

*University of Windsor*

Follow this and additional works at: <https://scholar.uwindsor.ca/etd>



Part of the [Electrical and Computer Engineering Commons](#)

---

### Recommended Citation

Saeid, Luca, "Underwater Source Localization based on Modal Propagation and Acoustic Signal Processing" (2021). *Electronic Theses and Dissertations*. 8860.

<https://scholar.uwindsor.ca/etd/8860>

This online database contains the full-text of PhD dissertations and Masters' theses of University of Windsor students from 1954 forward. These documents are made available for personal study and research purposes only, in accordance with the Canadian Copyright Act and the Creative Commons license—CC BY-NC-ND (Attribution, Non-Commercial, No Derivative Works). Under this license, works must always be attributed to the copyright holder (original author), cannot be used for any commercial purposes, and may not be altered. Any other use would require the permission of the copyright holder. Students may inquire about withdrawing their dissertation and/or thesis from this database. For additional inquiries, please contact the repository administrator via email ([scholarship@uwindsor.ca](mailto:scholarship@uwindsor.ca)) or by telephone at 519-253-3000ext. 3208.

**Underwater Source Localization based on Modal Propagation  
and Acoustic Signal Processing**

By

**Luca Saeid**

A Thesis

Submitted to the Faculty of Graduate Studies

through the Department of Electrical and Computer Engineering

in Partial Fulfillment of the Requirements for

the Degree of Master of Applied Science

at the University of Windsor

Windsor, Ontario, Canada

2021

© 2021 Luca Saeid

**Underwater Source Localization based on Modal Propagation  
and Acoustic Signal Processing**

by

Luca Saeid

APPROVED BY:

---

J. Ahamed

Department of Mechanical, Automotive & Materials Engineering

---

M. Hassanzadeh

Department of Electrical and Computer Engineering

---

S. Erfani, Co-Advisor

Department of Electrical and Computer Engineering

---

S. Alirezaee, Co-Advisor

Department of Electrical and Computer Engineering

June 24, 2021

## DECLARATION OF ORIGINALITY

I hereby certify that I am the sole author of this thesis and that no part of this thesis has been published or submitted for publication.

I certify that, to the best of my knowledge, my thesis does not infringe upon anyone's copyright nor violate any proprietary rights and that any ideas, techniques, quotations, or any other material from the work of other people included in my thesis, published or otherwise, are fully acknowledged in accordance with the standard referencing practices. Furthermore, to the extent that I have included copyrighted material that surpasses the bounds of fair dealing within the meaning of the Canada Copyright Act, I certify that I have obtained a written permission from the copyright owner(s) to include such material(s) in my thesis and have included copies of such copyright clearances to my appendix.

I declare that this is a true copy of my thesis, including any final revisions, as approved by my thesis committee and the Graduate Studies office, and that this thesis has not been submitted for a higher degree to any other University or Institution.



## ABSTRACT

Acoustic localization plays a pivotal role in underwater vehicle systems and marine mammal detection. Previous efforts adopt synchronized arrays of sensors to extract some features like direction of arrival (DOA) or time of flight (TOF) from the received signal. However, installing and synchronizing several hydrophones over a large area is costly and challenging. To tackle this problem, we use a single-hydrophone localization system which relies on acoustic signal processing methods rather than multiple hydrophones. This system takes modal dispersion into consideration and estimates the distance between sound source and receiver (range) based on dispersion curves. It is shown that the larger the range is, the more separable the modes are. To make the modes more distinguishable, a non-linear signal processing technique, called warping, is utilized.

Propagation model of low-frequency signals, such as dolphin sound, is well-studied in shallow water environment (depth  $D < 200$  m), and it was demonstrated that at large ranges (range  $r > 1$  km), modal dispersion is utterly visible at time frequency (TF) domain. We used Pekeris model for the aforementioned situation to localize both synthetic and real underwater acoustic signals. The accuracy of the localization system is examined with various sounds, including impulsive signal, sounds with known Fourier transform, and signals with estimated source phase. Experimental results show that the warping technique can considerably lessen the localization error, especially when prior knowledge about the source signal and waveguide are available.

## DEDICATION

I dedicate my dissertation work to my family, wife and many friends. A special feeling of gratitude to my loving parents, Karim Saeid and Afsaneh Aghabagheri for their endless love and encouragement. They have instilled in me a tireless work ethic and persistent determination to be whatever I wanted to be in life without limitations.

I also dedicate this dissertation to my amazing wife, Andrea Saeid, whose sacrificial care for our children and me gave me the courage, strength and consequently made it possible for me to complete this work; and our two daughters, Sophia and Ayla who made me keen on learning and who are indeed a treasure from the lord.

I dedicate this work and give special thanks to my brother, Shahab Saeid for his overwhelming support throughout this process. I will always appreciate all he has done for me, especially the phone calls and occasional visits since we reside in different countries. I am forever thankful for sharing your words of advice and encouragement to finish this study.

## ACKNOWLEDGMENT

I would like to sincerely thank my co-supervisor, Dr. Shahpour Alirezaee, for his guidance and support in successfully completing my thesis. I am deeply grateful for his involvement, guiding, mentoring and providing any help that I needed to complete my degree. It is an honor to have worked under his supervision.

I am grateful to my co-supervisor, Dr. Shervin Erfani, for his support and valuable comments which helped in completing this thesis.

I would also like to thank my committee members, Dr. Jalal Ahamed and Dr. Mohammad Hassanzadeh for their encouragement, constructive comments and positive criticism which in fact, improved my ideas and solutions.

Finally, I thank Dr. Saeed Mozaffari for helpful discussions and feedback.

## TABLE OF CONTENTS

<b>DECLARATION OF ORIGINALITY.....</b>	<b>iii</b>
<b>ABSTRACT.....</b>	<b>iv</b>
<b>DEDICATION.....</b>	<b>v</b>
<b>ACKNOWLEDGEMENTS.....</b>	<b>vi</b>
<b>LIST OF FIGURES.....</b>	<b>ix</b>
<b>LIST OF TABLES.....</b>	<b>xi</b>
<b>LIST OF ABBREVIATIONS/SYMBOLS.....</b>	<b>xiii</b>
<b>Chapter 1: Introduction.....</b>	<b>1</b>
1.1 Underwater Acoustics Applications.....	2
1.2 Objectives and Motivations.....	3
1.3 Challenges.....	3
1.4 Contributions.....	4
1.5 Outline of the Thesis.....	4
<b>Chapter 2: State of the Art.....</b>	<b>6</b>
2.1 Underwater Localization Systems.....	6
2.2 Acoustic Localization .....	7
2.3 Sound Propagation Model.....	10
2.4 Summary.....	15

<b>Chapter 3: Acoustic Signal Processing.....</b>	<b>16</b>
3.1 linear-time-invariant system .....	16
3.2 Fourier Transform .....	18
3.3 Time-Frequency representations .....	20
3.4 Dynamic mode decomposition Frequency representations .....	20
3.5 Warping Theory.....	25
3.6 Summary.....	28
 <b>Chapter 4: Literature Review.....</b>	 <b>29</b>
4.1 Data-driven methods.....	29
4.2 Model-based methods.....	33
4.3 Summary.....	37
 <b>Chapter 5: Dispersion-based Acoustic Source Localization.....</b>	 <b>38</b>
5.1 Discrete warping.....	38
5.2 Impulse signal warping.....	40
5.3 Known signal warping.....	43
5.4 Unknown signal warping.....	45
5.5 Modal filtering.....	46
5.6 Dispersion curve estimation.....	46
5.7 Range estimation.....	52
5.8 Depth estimation.....	52
5.9 Summary.....	55

<b>Chapter 6: Experimental Results.....</b>	<b>56</b>
6.1 Localization using synthetic data.....	56
6.2 Localization using real data.....	63
6.3 Summary.....	55
 <b>Chapter 7: Conclusion.....</b>	 <b>70</b>
7.1 Summary.....	70
7.2 Conclusion.....	70
7.3 Future work.....	70
 <b>REFERENCES/BIBLIOGRAPHY.....</b>	 <b>72</b>
<b>VITA AUCTORIS.....</b>	<b>78</b>

## LIST OF FIGURES

Figure. 2.1: Long baseline localization system .....	8
Figure. 2.2: Short baseline positioning system.....	9
Figure. 2.3: Ultra short baseline positioning system.....	10
Figure. 2.4: Shallow water sound propagation model.....	11
Figure. 2.5: Dispersion curves of the first five modes.....	13
Figure. 2.6: Group and phase velocities calculation.....	13
Figure. 2.7: The Pekeris waveguide schematic.....	14
Figure. 2.8: Signal propagation in a Pekeris waveguide.....	15
Figure. 3.1: System representation of a remote sound sensing application.....	16
Figure 3.2: Fourier representation.....	19
Figure 3.3: Signal reconstruction.....	19
Figure 3.4: Time filtering window in Gabor transform.....	20
Figure 3.5: Mather wavelet and two child wavelets.....	21
Figure 3.6: Different time-frequency representation methods.....	22
Figure 3.7: Spectrogram representation of a signal.....	23
Figure 3.8: Overview of the dynamic mode decomposition algorithm.....	24
Figure 3.9: A spatiotemporal signal and its modes.....	25
Figure 3.10: Comparison between different mode decomposition methods.....	25
Figure 3.12: Comparison between linear and non-linear time warping methods.....	27
Figure 4.1: Overview of the acoustic localization techniques.....	29
Figure 5.1: Sensitivity of warping and unwarping algorithms.....	40
Figure 5.2: Sensitivity of warping algorithm to range parameter. ....	40
Figure 5.3: A train of impulse signal. ....	41
Figure 5.4: Uncertainty in the time origin. ....	42

Figure 5.5: Spectrograms of different warping signals. ....	42
Figure 5.6: Spectrograms of different warping signals. ....	44
Figure 5.7: Effect of source deconvolution on warping. ....	44
Figure 5.8: Effect of phase compensation on warping. ....	45
Figure 5.9: Warping robustness to the source signal phase estimation.....	47
Figure 5.10: Filtering mask.....	48
Figure 5.11: Filtering process .....	48
Figure 5.12: Theoretical dispersion curves of the first four modes .....	49
Figure 5.13: Estimated dispersion curves of the first four modes .....	50
Figure 5.14: Comparison between theoretical and estimated dispersion curves.....	51
Figure 5.15: Modal dispersion curve restriction .....	51
Figure 5.16: Overall flowchart of the proposed acoustic localization technique .....	54
Figure 6.1: Experimental configuration .....	57
Figure 6.2: Sound signal localization .....	57
Figure 6.3: Noise effect on the modal separation .....	59
Figure 6.4: Noise effect on range estimation error .....	60
Figure 6.5: Effect of source/receiver distance on range estimation error .....	61
Figure 6.6: Range estimation error as a function of source/receiver distance .....	61
Figure 6.7: Range estimation error as a function of sea sound speed.....	62
Figure 6.8: Impulsive signal in real world.....	64
Figure 6.9: The effect of time origin selection on warped signal.....	64
Figure 6.10: Localization result for real impulsive signal.....	65
Figure 6.11: Real world signal in time domain.....	66
Figure 6.12: Received signal in TF domain.....	66
Figure 6.13: Calculated and estimated dispersion curves.....	67



Figure 6.14: Dolphin sound signal.....	68
Figure 6.15: Effect of phase compensation on a real signal.....	68
Figure 6.16: Localization result for a dolphin signal.....	69

## LIST OF TABLES

Table 6.1: Results of range estimation for different number of modes .....	58
Table 6.2: Results of range estimation for mode couples .....	58
Table 6.3: Compares between the Pekeris and Multipath models .....	63

## LIST OF ABBREVIATIONS/SYMBOLS

<b>Abbreviations/Symbols</b>	<b>Description</b>
DOA	Direction of Arrival
TOF	Time of Flight
TF	Time-frequency
UV	Underwater vehicle
GPS	Global positioning system
DR	Dead-Reckoning
INS	Inertial Navigation Systems
GN	Geophysical Navigation
SONAR	Sound Navigation and Ranging
LBL	Long Baseline
SBL	Short Baseline
USBL	Ultra-Short Baseline
LTI	Linear and time invariance
FT	Fourier transform
IFT	Inverse Fourier transform
TFR	Time-frequency representation
GT	Gabor transform
STFT	Short- time Fourier transform
WT	Wavelet transform
DMD	Dynamic mode decomposition
PCA	Principal Component Analysis
ICA	Independent Component Analysis

SVM	Support Vector Machine
DNN	Deep Neural Network
FrFT	Fractional Fourier Transform
LFM	linear frequency modulated
IoUT	Internet of Underwater Things
RL	Reinforcement-learning
RF	Random forests
CNN	Convolutional Neural Network
UWSN	Underwater wireless sensor networks
GLS	Generalized least squares
GRNN	Generalized regression neural network
SCM	Sample covariance matrix
SVR	Support vector regression
HRTF	Head-related transfer functions
GPR	Gaussian process regression
ASN	Acoustic sensor network
UASN	Underwater acoustic sensor networks
TOA	Time of arrival
BPSK	Binary Phase Shift Keying
BAOA	Bearing-angle-of-arrival
RSS	Received signal strength
MFP	Match field processing
MUSIC	Multiple signal classification

# CHAPTER 1

## Introduction

Covering more than 70% of the surface area of the earth, oceans have far-reaching impacts on the humans' life. They influence weather and climate, provide us food resources, and contain renewable energy. Underwater acoustics applications have been emerged to better understand the oceans and harness their unlimited potentials. These applications can be regarded as a remote sensing problem, where underwater acoustic signals reflected and emitted at a distance are detected and monitored [1]. Underwater acoustic applications can be broadly classified into four major categories: detection, classification, localization, and tracking.

In this thesis, we focus on *localization* application that aims to estimate the location of the object of interest based on sonar (*sound navigation and ranging*) system. Signal processing is the corner stone of the sonar systems as it converts underwater acoustic signals into navigation and ranging information. These systems typically consist of an array of sensors (called hydrophones) converting acoustic pressure underwater to an electrical voltage. Like a microphone that senses acoustic waves in air, a hydrophone captures sound signals in the water. To improve localization performance, most of sonar systems rely on multiple hydrophones that are configured in geometric patterns. Since installing several hydrophones on the seabed over a large area is an expensive and time-consuming task, single-hydrophone processing methods for sound source localizing have received much attention in recent years [2][3][4]. However, single sensor source localization is a challenging task, which requires not only specific acoustic signal processing techniques but also accurate knowledge of the underwater environment. This thesis is aimed at

leveraging non-linear signal processing methods and wave dispersion model for underwater sound source localization.

## **1.1 Underwater Acoustics Applications**

Underwater acoustic signal processing has a wide range of application, ranging from military to civilian [5]. Underwater vehicle (UV) navigation, fish and marine mammal finding, underwater communication, underwater environment study, are some of applications of underwater acoustics.

From a signal-processing perspective, underwater acoustics applications can generally be categorized into four groups: detection, classification, localization, or tracking.

- Detection can be considered as a binary hypothesis test, determining if a received signal is the signal of interest or if it is simply background noise. Marine mammal presence based on the received sound is an example of detection.
- Classification is a multiple hypothesis test which aims to assign a detected signal to a finite set of classes. For example, different types of whales can be classified according to their sounds.
- Localization can be regarded as an estimation problem that endeavors to find the location of the object of interest. In the localization application, for instance, we are interested to find out the position of a whale according to the received sound by the hydrophone.
- Tracking is combination of estimation and prediction. In other words, we not only interested in the location of the object of interest, but we want to know its location in the future. For example, from location and speed of a whale, its location at some time in the future can be predicted by the tracking algorithm.

## 1.2 Objectives and Motivations

This thesis is aimed at localization problem in the underwater environment based on sonar system. That is to say, the main objective of this research is to estimate the location of a sound source based on modal propagation and dispersion model in underwater environment.

Most traditional methods in ocean acoustic rely on multiple hydrophones which require to be synchronized to measurements of relative arrival times between these sensors. Moreover, array of sensors installation to cover large areas is awkward and expensive. These challenges motivated us to deploy an acoustic signal processing that entail only one hydrophone for localizing. To achieve this goal, however, advanced signal processing methods as well as accurate information about sound propagation in the test environment are needed.

## 1.3 Challenges

Single-hydrophone processing method for sound source localization is a challenging task, as it is based on mathematical models. Unlike sensor array methods which require simple calculations to measure time of arrival (TOA) [6] or direction of arrival (DOA) [7], a single-hydrophone acoustic system requires non-linear signal processing methods to decompose multipath information from the received signal. The extracted hidden features will be used by other algorithms to localize the transient sound source. The second challenge is that prior information about the environmental through which the sound propagates should be available. To address this issue, we assume the underwater environment is shallow water ( $D < 200\text{m}$ ), and emitted sound has low frequency ( $f < 500\text{Hz}$ ). This is due to fact that under above conditions, acoustic propagation can be accurately modeled using normal mode theory and modal propagation [8].

## 1.4 Contributions

(1) In this thesis, we used non-linear signal processing techniques to localize an underwater sound signal. Since this approach is model-based and exact characteristics of underwater environment should be known beforehand, different waveguides were examined. We studied two different shallow water model, Pekeris model, and underwater waveguide with reflective boundaries.

(2) Different underwater sound signals had been used to verify the localization system. In this study, we utilized both synthetic and real-world signals. These signals can be categorized into three groups: impulsive signal, signal with known waveform, and signal with unknown waveform. For each type, different preprocessing techniques was used to filter the modes more accurately.

(3) The localization accuracy was studied under different circumstances. For example, the effect of number of modes, noise strength, and waveguide parameters had been studied.

## 1.5 Outline of Thesis

The structure of this thesis is as follows:

- **Chapter 2** explains different types of underwater localization systems. It describes the underwater waveguide, Pekeris model, and sound propagation phenomenon in it. This chapter also mathematically presents fundamental concepts like group and phase velocities which cause modal dispersion.
- **Chapter 3** reviews acoustic signal processing methods. Various time-frequency signal representation approaches, such as Gabor transform, wavelet transform, and spectrogram



will be described in this chapter. Finally, warping technique that is the corner stone of this thesis will be explained.

- **Chapter 4** reviews signal processing based acoustic underwater localization methods. Data-driven and model-based methods will be explained in detail.
- **Chapter 5** explains the proposed dispersion-based acoustic source localization. The effect of warping technique on different signals will be explored. We will also illustrate dispersion curve estimation, and modal filtering. Finally, range estimation based on the comparison between calculated and estimated dispersion curve will be explained.
- **Chapter 6** presents experimental results and discusses the effect of different parameters on the localization accuracy.
- **Chapter 7** concludes the thesis by summarizing our contributions and making suggestions for future research.

## CHAPTER 2

### State of the Art:

This chapter begins by overviewing the main underwater navigation systems. Then, acoustic localization methods will be presented in more details, and different topologies will be compared. Plus, modal propagation in an acoustic waveguide will be mathematically described. Finally, State-of-the-art techniques for acoustic localization will be reviewed at the end of this chapter.

### 2.1. Underwater Localization Systems

As stated earlier, localization systems aim to estimate the position of the object of interest in its surrounding environment. It is worth mentioning that global positioning system (GPS), the most accessible technique for localization, cannot be deployed in underwater environment, because relatively weak GPS signals considerably attenuated and do not penetrate far distances on water. Therefore, underwater localization systems rely on other sensors such as compass, gyroscopes, camera, sonar, and accelerometer. Based on the employed sensors, underwater localization methods can typically be classified into four major groups [9].

- The earliest and simplest localization method include *Dead-Reckoning* (DR) and *Inertial Navigation Systems* (INS) which is based on gyroscope and accelerometer that measures water-speed and the object of interest's velocities according to physical laws. Although DR/INS method is suitable for localization over long-range missions, its position accuracy declines over time.
- To compensate the accuracy drifts of the DR/INS system, *Geophysical Navigation* (GN) system has been proposed. GN rely on magnetic and gravimeter sensors and requires geophysical maps to match it with the sensors data. Dependency on previously generated maps and high computation for data matching are main drawbacks of this system.
- *Optical systems* is another common localization method. They employ camera and light detector to obtain underwater images and recognize landmarks. Underwater environments suffer from inadequacy of lighting, resulting in low quality images, especially in high depth areas. These challenges severely curtail the application of optical localization systems.

- To tackle this problem, *acoustic* localization systems have been emerged which rely on sound signals. Sonar system is the most popular acoustic method that make use of acoustic equipment such as beacon, hydrophone, and transponder to emit and receive sound signals. While beacon emits a predefined sound signal periodically, hydrophone receives emitted signal. Transponder can be considered as a combination of beacon and hydrophone, as it is able to receive and emit sound signals concurrently. When transponder receives a signal with specific frequency, it sends a signal in response.

Some take advantage of the complementary nature of the above sensors and combine them to minimize the localization error [10]. This technique, called sensor fusion, improves the localization accuracy but at the expense of higher cost. In this thesis we focus on the acoustic localization based on single-hydrophone method, because multiple hydrophones installation is relatively expensive. Consequently, to minimize the cost of the localization system, fewer hydrophones should be deployed. Recent work has demonstrated how a single hydrophone can be used to sound amplitude estimation in underwater environment [11].

## **2.2. Acoustic Localization**

Acoustic signals have been used more frequently for underwater localization and communication as they penetrate deeper in water, compared with other signals, such radio and electromagnetic. Some of the acoustic-based methods are Sound Navigation and Ranging (SONAR) and acoustic ranging.

### **2.2.1. Sonar**

Sonar is a technique that uses sound propagation for underwater vehicles navigation and communication. In terms of localization, sonar systems can estimate the location of object of interest either actively or passively. In *active* sonar, acoustic pulses are transmitted and their echoes from other objects are captured. Based on the speed of sound in water and time difference between transmitting and receiving sound signals, location of surrounding objects can be determined. In the presence of several objects, active sonar receives multiple echoes, making localization process more challenging. In contrast to active sonar, *passive* sonar makes use of hydrophones to listen to the generated sounds from other objects.

### 2.2.2. Acoustic Ranging

Acoustic ranging systems have been used for underwater vehicles (UV) localization and navigation [12]. These systems rely on communication between an acoustic transmitter and a set of hydrophones, called baseline. If the sound velocity is known in underwater, the distance between transmitter and hydrophones can be estimated by simple geometric relationships. Based on the position and arrangement of acoustic equipment, acoustic ranging systems can be categorized into: Long Baseline (LBL), Short Baseline (SBL) and Ultra-Short Baseline (USBL) [9].

- **Long Baseline (LBL)**

This method uses some hydrophones, installed on the seabed and one transmitter that is fixed to the UV. Figure 2.1 shows LBL configuration. First, the transmitter propagates an acoustic signal. After receiving this signal by the active hydrophones, they transmit another signal in response. The distance between the UV and each transponder can be calculated, based on the time difference between transmitted and received sound signals. To find the exact position of the UV, triangulation method is used [13]. The main advantage of LBL is its high localization accuracy which is in the range few centimeters over a wide area. However, since transponder beacons should be installed on the seabed, this method is costly and time-consuming to be set up [14].

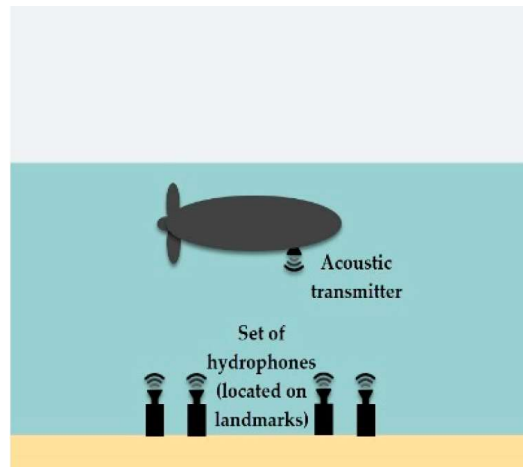


Figure. 2.1: Long baseline localization system [9].

- **Short Baseline (SBL)**

In SBL localization method, hydrophones are mounted far from each other on a floating platform like a boat (Figure 2.4). It is shown that the distance between hydrophones severely affects the localization accuracy; that is to say, the longer the distance, the lower the localization error. The baseline length is usually in the range of several meters. SBL works by measuring a relative position between the reference sound source and the receiving array.

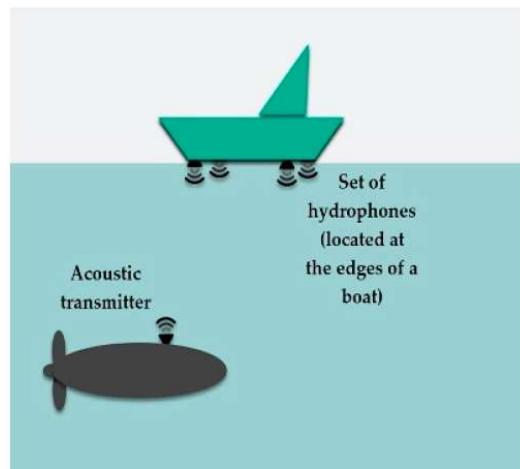


Figure. 2.2: Short baseline positioning system [9].

- **Ultra Short Baseline (USBL)**

As Figure 2.5 shows, USBL localization method is similar to SBL, but hydrophones are closely spaced with the approximated distance on the order of centimeter. Unlike SBL method, USBL measures the phase differences between received sound signals by the sensor array. Both SBL and USBL methods rely on a floating platform to install transponders, which is not always possible. Localization accuracy of SBL depends on the dimensions of the floating platform, and it seemingly declines when it comes to short mothership.

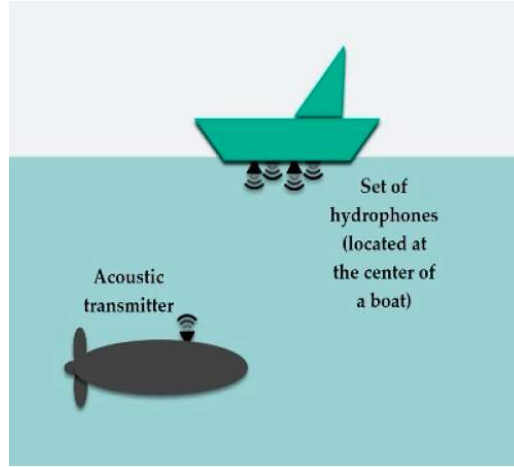


Figure. 2.3: Ultra short baseline positioning system [9].

### 2.3. Sound Propagation Model

Acoustic localization systems should be aware of the sound propagation mechanism in underwater to be able to calculate the location of the object of interest. The speed of sound in underwater usually varies between 1440 m/s and 1550 m/s, depending on the pressure, salinity and temperature of water [15]. Acoustic signals are attenuated and lose their power when traveling in underwater environment. Ambient noise also affects the strength of the passing acoustic signal. Acoustic noise is usually modeled as a Gaussian noise with power spectral density decaying at around 18 dB per decade [15]. The received sound frequency changes due to motion of either sound source or sound receiver, which is called Doppler effect. This frequency shift is aggravated by the low speed of the sound [16].

These variations in the amplitude and frequency of the sound through its propagation in the underwater environment makes acoustic sound analysis more tricky. To cope with this situation, we assume that underwater environment is a shallow water ( $D < 200$  m) and sound signal has a low-frequency ( $f < 500$  Hz). This is due the fact that in shallow-water, especially for long-range sound transmission (range  $r > 1$  km), the underwater environment can be regarded as a dispersive medium in which sounds with different frequencies travel with different velocities [17]. This frequency-dependent arrival of sound signals causes the received signal to be made of several components, called *modes*. It has been shown that under low-frequency and shallow water assumptions, acoustic propagation can be accurately modeled by *modal propagation* [18]. Shallow water environment can be regarded as an acoustic waveguide with multipath

propagation as it is highly influenced by the sea surface and the seabed reflections. Some modes might travel by a more direct path, and arrive sooner than modes that reflected at the sea surface or sea bottom. Because of the arrival of different modes of the signal at different times, the hydrophone receives a distorted form of the sound. Figure 2.4 shows a multipath propagation acoustic waveguide [19].

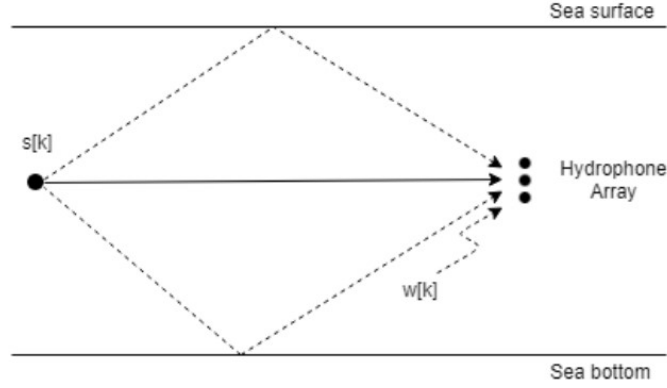


Figure. 2.4: Shallow water sound propagation model [19].

### 2.3.1 Modal Propagation

As mentioned earlier, in shallow water the sound signal is spread in time because the propagation velocity is dependent on the frequency and it is not equal for all modes. Assume a sound source  $S(f)$  at depth  $Z_s$  that transmits sound signal with frequency  $f$ . The received signal by a hydrophone at depth  $Z_r$  at range  $r$  is as follows [17]:

$$y(f, Z_s, Z_r) = s(f)g(f, Z_s, Z_r, r) \quad (2-1)$$

Where  $g$  is the impulse response of the shallow water environment. According to normal mode theory, each mode propagating dispersively and the received sound at ranges greater than acoustic wavelengths is the sum of several modal components. By solving the acoustic wave equation using the classic separation of variables method we can derive [19]:

$$g(f, Z_s, Z_r, r) = \sum_{m=1}^M a_m(f, Z_s, Z_r) e^{j\phi_m(f, r)} \quad (2-2)$$

where  $M$  is the number of modes, each having an amplitude  $a_m(f, Z_s, Z_r)$  and phase  $\phi_m(f, r)$ . The speed of each mode is called *phase velocity* and we refer to the speed of the overall pattern, consisting of different modes, as the *group velocity*. Equation (2-2) shows that only modal phase

and consequently mode travel time (phase velocity) depends primarily on the range ( $r$ ). In other words, modal amplitude is independent of the distance between source and receiver and only varies with their depth.

Therefore, in acoustic localization application, modal phase is of paramount importance as it includes valuable information about the range parameter. It is shown that modal phase can be regarded as a separable function of two independent variables [18]:

$$\phi_m(f, r) = rk_m(f) \quad (2-3)$$

where  $k_m(f)$  is the spatial frequency of mode  $m$ , which depends on the environment, but not on the experimental geometry. That is to say, only environment parameters such as water depth, and sound speed profile affect the modal spatial frequency. Therefore, the travel time of each mode is:

$$t_m(f) = \frac{1}{2\pi} \frac{\partial \phi_m(f, r)}{\partial f} = \frac{r}{v_m(f)} \quad (2-4)$$

The above equation indicates that the modal travel time depends on range  $r$  and modal group speed  $v_m(f)$ . If the sound source be  $s(f) = |s(f)|e^{\phi_s(f)}$ , according to equations (2-1) and (2-2), the received sound signal will be:

$$g(f, Z_s, Z_r, r) = \sum_{m=1}^M |s(f)| a_m(f, Z_s, Z_r) e^{j[\phi_m(f, r) + \phi_s(f)]} \quad (2-5)$$

So, the received phase becomes  $\phi_m(f, r) + \phi_s(f)$ . According to equation (2-4), the modal travel times for a general received signal become:

$$t_m(f) = \frac{1}{2\pi} \frac{\partial [\phi_m(f, r) + \phi_s(f)]}{\partial f} = t_s(f) + \frac{r}{v_m(f)} \quad (2-6)$$

where  $t_s(f)$  is the source time frequency law, and  $v_m(f)$  is the source *group delay* of the received mode  $m$ . Unlike phase delay that shows the time delay of a single mode, group delay is a measure of amplitude distortion when multiple components with different frequencies construct the overall signal. In other words, while phase velocity is the speed of each mode, group velocity is the speed of the overall signal consists of all modes.



Equation (2-6) is called *dispersion curve* and it gives mode's location in the time-frequency (TF) domain. Dispersion occurs when modals with different frequencies propagate at different speeds. In other words, in a dispersive medium, group velocity ( $v_g$ ) and phase velocity ( $v_p$ ) are not equal. Figure 2.6 shows the group and phase velocities for  $y(x, t) = A\cos(\omega t - kx)$  signal.

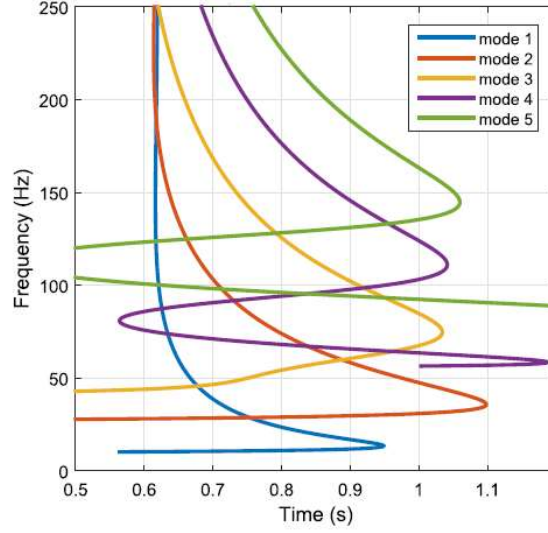


Figure. 2.5: Dispersion curves of the first five modes [17].

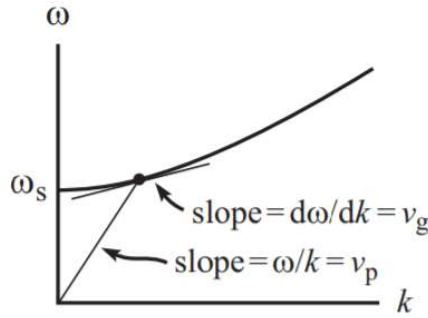


Figure. 2.6: .

### 2.3.2. Pekeris Waveguide

To analyze modal propagation and generate simulated signals, a simple model of shallow water environment, called Pekeris waveguide, will be utilized in this thesis. Pekeris waveguide has been used frequently to model coastal environments for acoustic signal processing [21][22]. This model assumes that the sound signal travels with the same speed in all directions in water (isocelocity property) between a perfectly reflecting surface (the sea surface) and a semi-infinite

isovelocity fluid basement (the seabed). Figure 2.7 shows the Pekeris waveguide. Although the model does not include any realistic parameters of the environment for the sake of simplicity, it produces accurate modal features. Having the parameters of its water column and seabed such as sound speed ( $C$ ), density ( $\rho$ ), and attenuation coefficient ( $\alpha$ ), Pekeris model can precisely simulate the sound propagation in shallow water environment ( $D < 200m$ ).

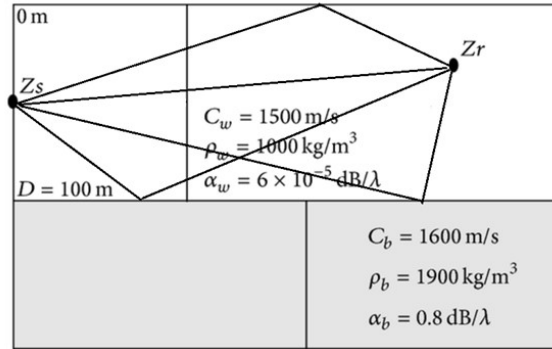


Figure 2.7: The Pekeris waveguide schematic [22].

By using the Pekeris model and simple numerical solvers [23], one can obtain modal travel time from equation (2-6) [24]. Figure 2.8 shows signal propagation phenomena, using Pekeris model. Figure 2.8 (a) shows the source signal that is a short broadband pulse with 0.1 s duration. Since modal group speed depends on frequency and source signal has frequencies within 25 Hz and 75 Hz, it experiences dispersion in the underwater environment. As state before, in a dispersive medium, different modes travel with different speeds, causing the received signal to have a wider duration compared with the source signal. According to equation (2-6), the larger the distance between sound source and receiver, the wider the received signal. One can see from figure 2.8 (b) that duration of the received signal is increased from 0.1s to 0.2s at 5 km range. As Figure 2.8 (c) illustrates, modal dispersion is more obvious when source/receiver range increases. At 15 km range, three modes are distinguishable. Mode 1 arrives between  $t > 0s$  to  $t < 0.20 s$ , while mode 2 arrives between  $t > 0.15s$  to  $t < 0.40 s$ . There is also a third mode, barely visible after  $t > 0.35 s$ .

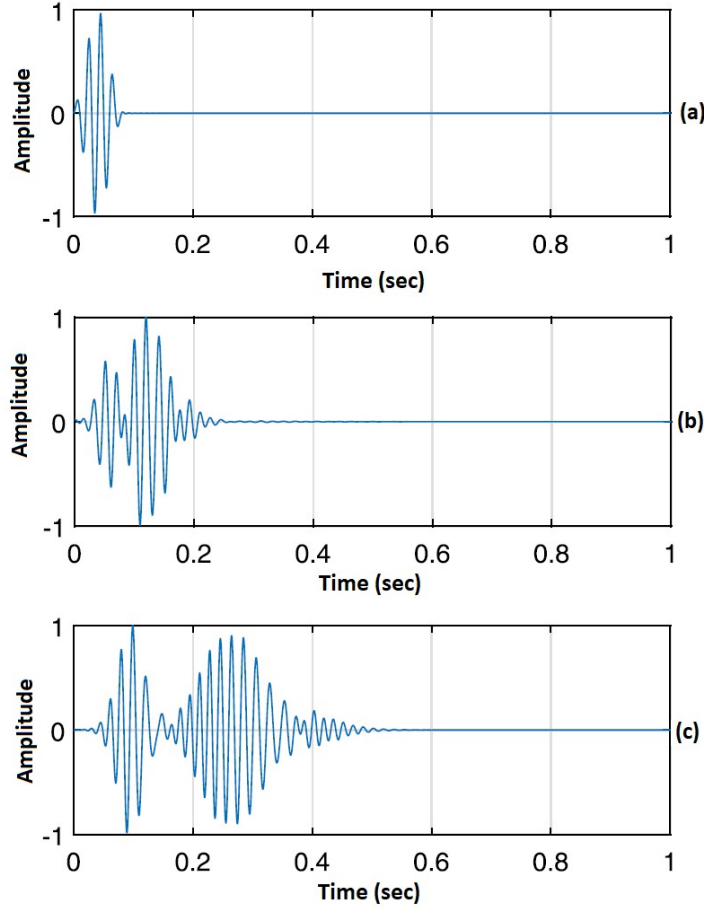


Figure. 2.8: Signal propagation in a Pekeris waveguide.  
(a): The sound source. (b): Received signal at  $r=5\text{km}$ . (c): Received signal at  $r=15\text{km}$ .

#### 2.4. Summary:

This chapter reviewed different underwater localization, and mainly focused on acoustic based localization. Then, Pekeris underwater waveguide and sound propagation through this channel were studied. Finally, modal dispersion in shallow water and dispersion curves were explained.

## CHAPTER 3

### Acoustic signal processing

This chapter presents different signal processing techniques required for underwater sound source localization. First, a linear-time-invariant system is defined because an underwater waveguide can be described as such a system. Then, Fourier transform that is the fundamental tool in signal processing is presented. Afterwards, different signal representation methods such as Gabor, wavelet, and spectrum will be discussed. Finally, we will present details of warping technique, which will be used for modal separation in this thesis.

#### 3.1. Linear-Time-Invariant system (LTI)

To leverage signal processing techniques for specific applications, physical environment affecting signals should be characterized and analyzed. In this thesis, for instance, we aim at sound localization application based on signal processing techniques. For this purpose, the underwater environment will be described as a system with an input signal ( $x(t)$ ) and an output signal ( $y(t)$ ), as shown in Figure. 3.1. In this case, the input signal would be the transmitted acoustic signal, and the output is the measured echoes. In general form, systems can have multiple inputs (e.g., signal and noise) and multiple outputs (e.g., several hydrophones at multiple points). A system with transfer function  $H$  mathematically converts the input signal to the output signal:

$$y(t) = H[x(t)] \quad (3-1)$$

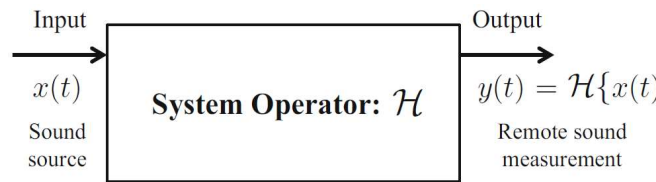


Figure 3.1: System representation of a remote sound sensing application.

For the sake of simplicity, many physical systems are assumed to be linear and time invariance (LTI). A system is called *linear* if for an input signal composed of distinct set of individual signals, the output will be a corresponding linear combination of the system output to each of the specific signals. A system is *time-invariant* if its characterization does not change over time.

That is to say, if an input signal is delayed by an arbitrary amount of time, the output signal experience an identical delay. In LTI systems, the output of any arbitrary signal can be obtained if the response of the system to the impulse signal is known. If the impulse response is denoted by  $h(t)$ , the output of the system to the input signal  $x(t)$  can be attained by convolution operator, represented by an asterisk (\*):

$$y(t) = x(t) * h(t) = \int_{-\infty}^{+\infty} h(\tau)x(t - \tau)d\tau \quad (3-2)$$

In our application, the acoustic signal  $x(t)$  propagates through multiple paths in the underwater channel (section 2.3). If the  $i^{th}$  path has an attenuation factor of  $a_i$  and delay of  $\tau_i$ , the received signal by the hydrophone located distance away would be:

$$y(t) = \sum_{i=1}^n a_i x(t - \tau_i) \quad (3-3)$$

The underwater waveguide can be assumed as a LTI system with the impulse response of  $h(t) = \sum_{i=1}^n a_i \delta(t - \tau_i)$ .

Sinusoidal signals are prevalent in underwater environment. Plus, they can simplify the input-output relationships of LTI systems. Assume a sinusoid input signal with frequency  $f_0$ . Using equation (3-2), the output will be:

$$\begin{aligned} y(t) &= H[e^{j2\pi f_0 t}] = \int_{-\infty}^{+\infty} h(\tau) e^{j2\pi f_0 (t-\tau)} d\tau \\ &= \left[ \int_{-\infty}^{+\infty} h(\tau) e^{-j2\pi f_0 \tau} d\tau \right] e^{j2\pi f_0 t} = [H(f_0)] e^{j2\pi f_0 t} \end{aligned} \quad (3-4)$$

The term  $H(f) = \int_{-\infty}^{+\infty} h(t) e^{-j2\pi f t} dt$  is the Fourier transform of the impulse response and it is called the *frequency response* of the system. The frequency response has a phase  $\angle H(f_0)$  and an amplitude of  $|H(f_0)|$ . Therefore, equation (3-4) can be written as:

$$y(t) = |H(f_0)| e^{j\angle H(f_0)} e^{j2\pi f_0 t} \quad (3-5)$$

The above equation shows that the response of a LTI system to a sinusoidal signal is another sinusoidal signal with the same frequency but different amplitude and phase due to system characteristics.

### 3.2. Fourier Transform

Fourier transform (FT) is an informative form for signal representation and has become an essential part of acoustic signal processing applications. FT is a mathematical transform that decomposes a signal in the time domain to the sum of sinusoidal functions and describes the frequency content of a time domain signal. The Fourier transform of the signal  $x(t)$  is:

$$X(f) = \int_{-\infty}^{+\infty} x(t) e^{-j2\pi ft} dt \quad (3-6)$$

Linear operations in time domain have corresponding operations in the frequency domain, which are sometimes easier to perform. A standout example is convolution operation in the time domain that equals to ordinary multiplication in the frequency domain. Therefore, equation (3-2) in the time domain can be represented in the frequency domain as follows:

$$Y(f) = H(f)X(f) \quad (3-7)$$

After performing the desired operations, inverse Fourier transform (IFT) should be used to convert the obtained result back to the time domain. Equation (3-8) shows the IFT.

$$x(t) = \int_{-\infty}^{+\infty} X(f) e^{j2\pi ft} df \quad (3-8)$$

The Fourier transform of  $x(t)$  is a complex-valued function of frequency, consisting of amplitude  $|X(f)|$  and phase  $\angle X(f)$ . The amplitude represents the relevant presence of a sinusoid, while the phase determines how the sinusoids should line up relative to one another to form the time domain signal. Both amplitude and phase of the FT have valuable information about the time domain signal. However, typically phase contains more information than amplitude. Figure 3.2 shows two 2-D signals (images) with their corresponding Fourier amplitudes and phases. Figure 3.3 illustrates the reconstruction process when amplitude or phase has been altered. If the amplitudes of the images remain the same but the phases were set to zero, the reconstructed images are not recognizable (Figure 3.3 (a)). On the other hand, the reconstructed images are still differentiable when the amplitudes were normalized to one, but the phases remained unchanged (Figure 3.3 (b)). Figure 3.3 is a testimony to the importance of phase information. It is worth mentioning that in the acoustic localization phase information is of paramount of importance because time delays of travelling sound signals is captured in the

phases of the received signals. Equation (3-9) shows that if a signal  $x(t)$  is delayed by  $\tau$ , its Fourier transform changes only in the phase.

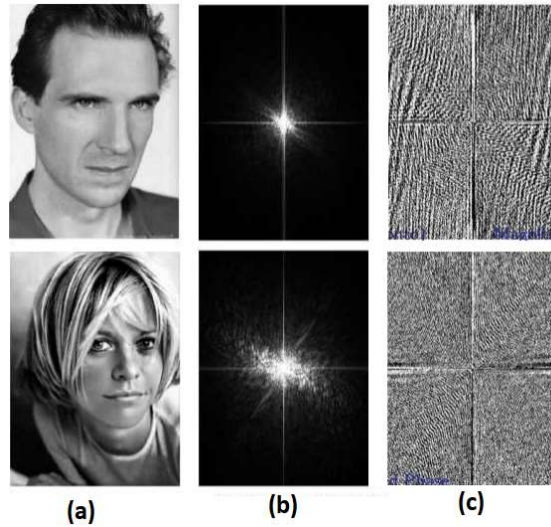


Figure 3.2: Fourier representation.  
(a): Original signals. (b): Fourier amplitudes. (c): Fourier phases.

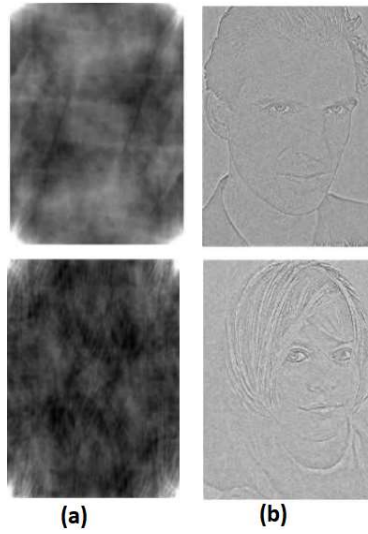


Figure 3.3: Signal reconstruction.  
(a): Remaining the amplitudes unchanged. (b): Remaining the phases unchanged.

$$\begin{aligned}
 F[x(t - \tau)] &= \int_{-\infty}^{+\infty} x(t - \tau) e^{-j2\pi ft} dt \\
 &= e^{-j2\pi f\tau} \int_{-\infty}^{+\infty} x(s) e^{-j2\pi fs} ds = e^{-j2\pi f\tau} X(f) \quad (3-9)
 \end{aligned}$$

### 3.3. Time-Frequency representations

Although Fourier transform captures the entire frequency content of the signal, it does not provide any information about the exact moment in time when these frequencies are presented. This is due to the fact that all time-domain information is ignored as FT is obtained by integrating over all time (equation 3-6). To address this issue, time-frequency representation (TFR) has been emerged [25]. TFR is extremely beneficial for analyzing time-varying signals, containing many components with variable amplitudes and/or frequencies. Since amplitudes of sound modals lessen when they travel in an underwater environment, we will use TFR in this thesis to analyze the signals. In the following, two prevailed TFRs will be explained.

#### 3.3.1. Gabor Transform (GT)

The Gabor transform, also known as the short- time Fourier transform (STFT), is one of the oldest linear TFRs [26]. Gabor modified the Fourier transform by introducing a new kernel to capture both time and frequency information.

$$g_{t,\omega}(\tau) = e^{i\omega\tau} g(\tau - t) \quad (3-10)$$

The function  $g(\tau - t)$  is centered at  $\tau$  with a fixed width and it acts as a time filter to indicate which frequencies are present over a specific window of time (Figure 3.4).

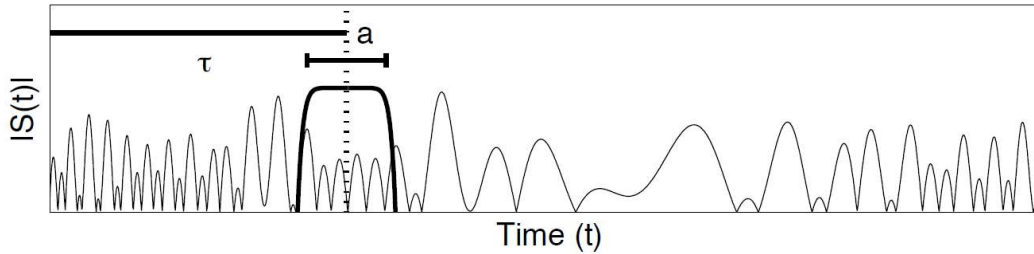


Figure 3.4: Time filtering window in Gabor transform [25].

The Gabor transform of the signal  $f(t)$  can be calculated as follows:

$$G_f(t, \omega) = \int_{-\infty}^{+\infty} f(\tau) \bar{g}(\tau - t) e^{-i\omega\tau} d\tau \quad (3-11)$$

where  $\bar{g}$  denotes the complex conjugate of the function  $g$ . The integration over the parameter  $\tau$  slides the time-filtering window to obtain the frequency information at each time interval.



Although the GT is able to pick out time and frequency information simultaneously, it has several shortcomings that stem from its fixed time-filtering window. If a portion of the signal has a wavelength longer than the window width, GT is not able to extract the information accurately. The second problem of GT is the trade-off between captured time and frequency information. If we shrink the time-filtering window, the less frequency information would be obtained. On the other hand, the longer the window, the less information there is concerning time content. To tackle these issues, wavelet transform has been proposed.

### 3.3.2. Wavelet Transform (WT)

Unlike GT that has a fixed-size filtering window, WT has an adjustable window (parameter  $a$  in Figure 3.4) to extract information in the time resolution more efficiently. Bearing in mind that time and frequency domains have a reverse relationship, the width of window is shortened to extract higher frequencies at better time resolution. On the other hand, to capture the low-frequency components of the signal, a broad scaling window can be utilized. To have a flexible filtering window, the following function, called mother wavelet, was introduced [26]:

$$\psi_{a,b}(t) = \frac{1}{\sqrt{a}} \psi\left(\frac{t-b}{a}\right) \quad (3-12)$$

where  $a$  and  $b$  are real constants that control the shape of the wavelet. The parameter  $a$  changes the scale and parameter  $b$  shows translation. Figure 3.5 illustrates the effect of controlling parameters on the mother wavelet ( $\psi_{1,0}$ ) shape and resulting child wavelets ( $\psi_{1/4,6}$ ,  $\psi_{3/2,-3}$ ).

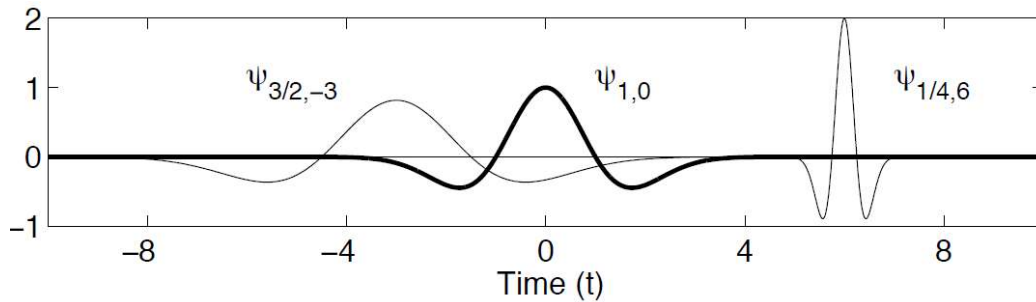


Figure 3.5: Mather wavelet and two child wavelets [25].

Wavelet transform of the function  $f(t)$  using mother wavelet  $\psi_{a,b}$  can be calculated as follows:

$$W_\psi[f](a, b) = \int_{-\infty}^{+\infty} f(t) \bar{\psi}_{a,b(t)} dt \quad (3-13)$$

To analyze the signal at different times and frequencies, the signal is first decomposed into a collection of smaller signals, by changing the translating factor ( $b$ ). Then, the original signal is processed at different frequency bands, by scaling the wavelet window with the scaling parameter ( $a$ ). Figure 3.5 compares different time-frequency representation methods. One can see that WT presents a multiresolution representation of the signals.

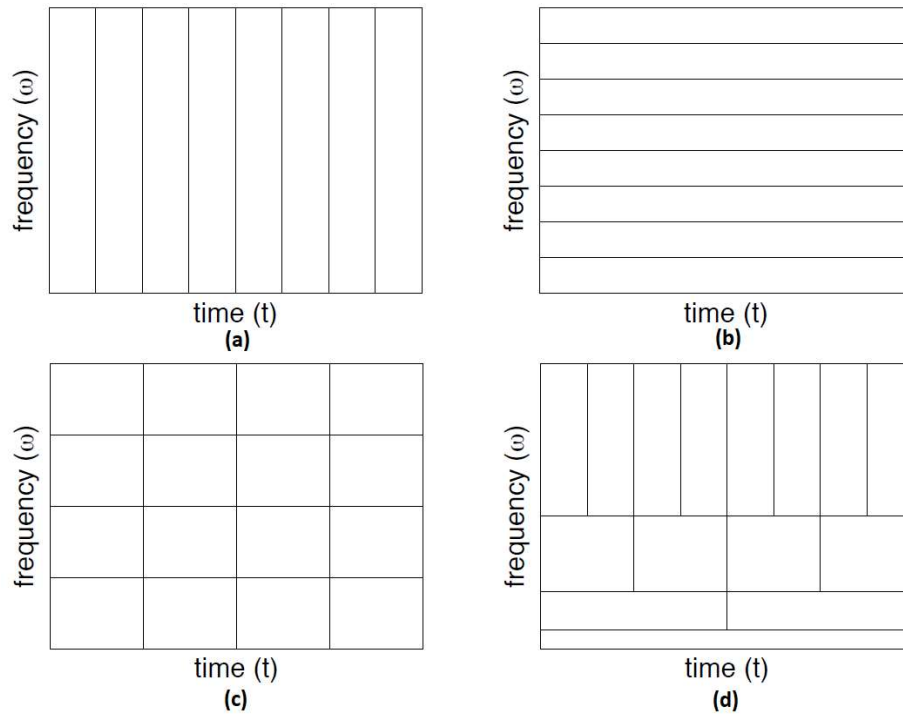


Figure 3.6: Different time-frequency representation methods [25].

(a): Time series. (b): Fourier. (c): Gabor transform. (d): Wavelet transform.

### 3.3.3. Spectrogram

Spectrogram is one of the most practical TF representations that has been used frequently in various applications such as sonar [27], radar [28], and speech [29] processing. It can be generated by Gabor transform or by a Wavelet transform. Assume Gabor transform, the squared magnitude of GT is called the spectrogram and is expressed as follows:

$$\text{Spectrogram}(t, \omega) = \left| \int_{-\infty}^{+\infty} f(\tau) \overline{g}(\tau - t) e^{-i\omega\tau} d\tau \right|^2 \quad (3-14)$$

To create the spectrogram, the signal is sampled in the time domain. In other words, the signal is divided into sections with overlap between contiguous sections. Then, Fourier transform is performed to calculate the magnitude of the frequency spectrum for each section. Each segment corresponds to a horizontal line in the spectrogram image. By putting these time plots side by side, spectrogram image is obtained. As it can be seen in Figure 3.7, spectrogram better represents the signal as four modes are clearly visible in Figure 3.7 (b).

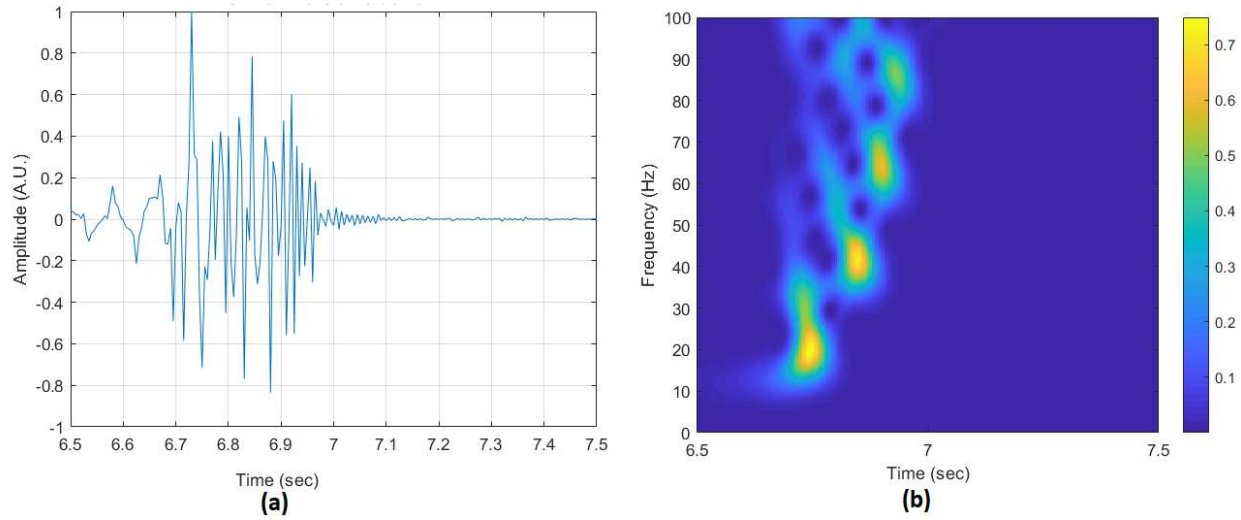


Figure 3.7: Spectrogram representation of a signal.  
(a): Signal in the time domain. (b): Spectrogram of signal (a).

### 3.4. Dynamic mode decomposition

Dynamic mode decomposition (DMD) is a data-driven approach which is used to discover complex dynamical systems [26]. Assume we have a dynamical system with two sets of data.

$$X = \begin{bmatrix} \vdots & \vdots & \vdots \\ X_1 & X_2 & \cdots & X_{m-1} \\ \vdots & \vdots & \vdots \end{bmatrix} \quad (3-15)$$

$$X' = \begin{bmatrix} \vdots & \vdots & \vdots \\ X'_2 & X'_3 & \cdots & X'_m \\ \vdots & \vdots & \vdots \end{bmatrix} \quad (3-16)$$

If  $F$  represents the dynamics of the system, then  $X_{k+1} = F(X_k)$ . By production the shifted data set ( $X'$ ) and the Moore–Penrose pseudoinverse of the data ( $X^\dagger$ ), the high-dimensional matrix  $A$  is obtained.

$$A = X'X^\dagger \quad (3-17)$$

It was shown that dynamic modes, are the eigenvectors of  $A$ , and each DMD mode corresponds to a particular eigenvalue of  $A$  [26]. Figure 3.8. shows the schematic overview of the dynamic mode decomposition algorithm.

Consider a spatiotemporal signal  $f(x, t)$  that is composed of two individual signals (modes)  $f_1(x, t)$  and  $f_2(x, t)$ .

$$f(x, t) = f_1(x, t) + f_2(x, t) = \text{sech}(x + 3) \exp(i2.3t) + 2 \text{sech}(x) \tanh(x) \exp(i2.8t) \quad (3-18)$$

According to Equation (3-18), the main signal has two modes with frequencies of  $\omega = 2.3$  and  $\omega = 2.8$ . Figure 3.9 shows the main signal and its components.

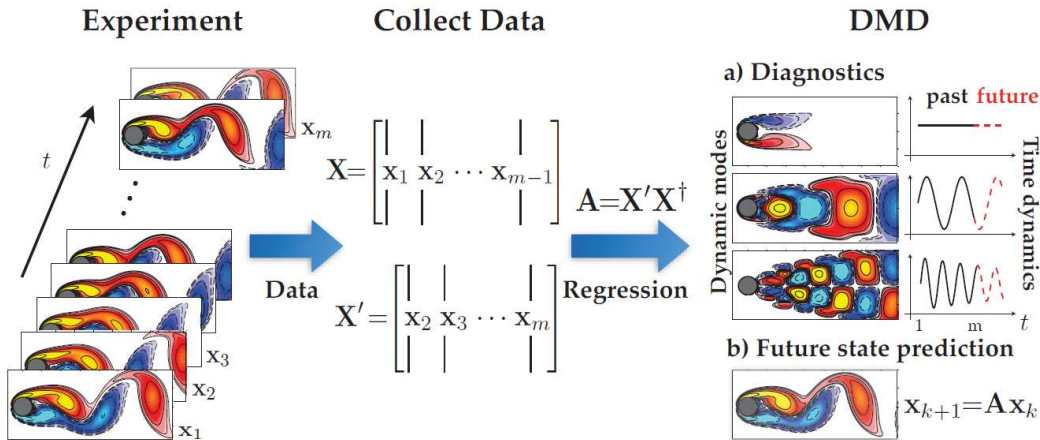


Figure 3.8: Overview of the dynamic mode decomposition algorithm [26].

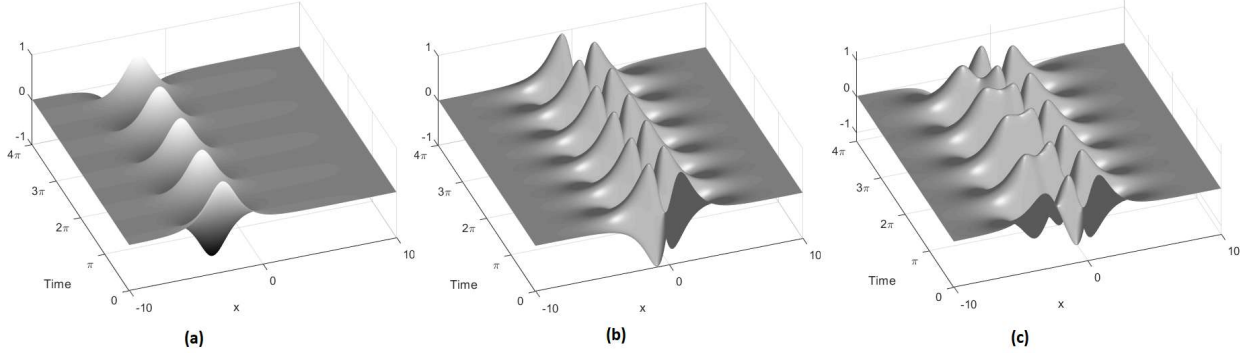


Figure 3.9: A spatiotemporal signal and its modes.  
(a): The first mode  $f_1(x, t)$ . (b): The second mode  $f_2(x, t)$ . (c): The main signal  $f(x, t)$ .

Figure 3.10 compares dynamic mode decomposition, Principal Component Analysis (PCA) [5], and Independent Component Analysis (ICA) [5] methods quantitatively. Spatial and temporal modes of the signal in Figure.3.9 (c) are extracted with DMD, PCA, and ICA methods and compared with their true values. According to Figure 3.10, the extracted modes by the DMD have the minimum error. While the PCA modes are very inaccurate, the ICA error is less than half the error associated with PCA. This comparison is a testimony to the DMD efficiency in decomposing spatiotemporal data.

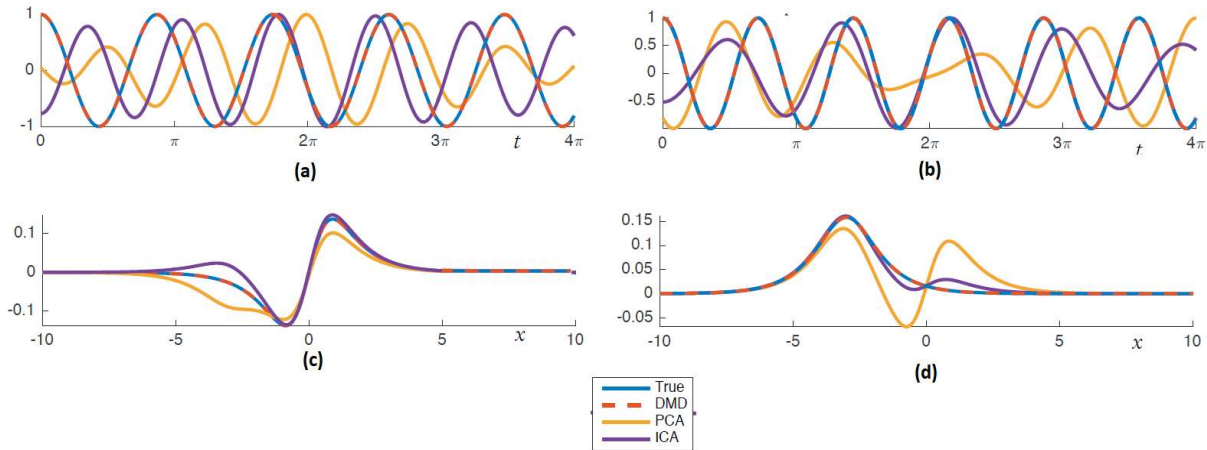


Figure 3.10: Comparison between different mode decomposition methods [5].  
(a): Mode 1 temporal. (b): Mode 2 temporal. (c): Mode 1 spatial. (d): Mode 2 spatial.

### 3.5. Warping theory

Hydrophones record the received sound signals as a function of time. Due to non-linear time dependence, modes with higher frequency arrive later at the hydrophone. Classical methods are not suitable to represent signals traveling in a non-linear medium. To address this issue, warping

technique has been employed to *linearize* the modes. After mode linearization, standard time-frequency methods, such as the spectrogram, can be utilized to represent the transformed signal. In other words, warping can be deployed to counteract or mitigate the non-linear effects of the ocean waveguide on the sound signals. To do this, the received signal should be compression or stretching over time. In this thesis, we aim to use warping to separate the modes more easily, which is a challenging task especially in short ranges where modes are highly convoluted. After modal separation, one mode will be filtered for sound source localization.

For a non-linear waveguide such as ocean environment, non-linear warping should be used. In contrast to linear signal compression or stretching (Figure 3.11 (b) and (c)), after non-linear warping the frequency of the warped signal varies with time (Figure 3.11 (d) and (e)). As it is clear in Figure 3.11 (e), frequency of the transformed signal is higher in 3s to 4s interval than 1s to 2s period. One can see that amplitude of the warped signal also changes over time, because energy of the signal should remain constant before and after warping transformation. To this end, the amplitude of the compressed signal in time must be increased to conserve energy.

From mathematical point of view, warping is substitution time  $t$  by  $h(t)$ , called a warping function. For the original signal  $y(t)$ , the warped signal  $y_w(t)$  can be obtained by the following [18]:

$$y_w(t) = \sqrt{|h'(t)|} y[h(t)] \quad (3-19)$$

The derivative of warping function is depicted by  $h'(t)$  and the term  $\sqrt{|h'(t)|}$  is used for energy conservation. Choosing an appropriate warping function is of the paramount of importance. Basically, the warping function should be reversible. This property guaranties that all points in the warped signal match uniquely to all points in the original signal. The one-to-one correspondence between all points in  $y(t)$  and  $y_w(t)$ , will enable us to perform the inverse warping after modal filtering to convert the mode of interest into original time domain. Consider a signal  $y(t) = a(t)e^{-i2\pi f_0 \Phi(t)}$  which has amplitude of  $a(t)$  and constant frequency of  $f_0$ . Assume that the signal has a non-linear phase  $\Phi(t)$ . To linearize the signal phase, the warping function should be the inverse of the phase function. By substituting the  $h(t)$  with  $\Phi^{-1}(t)$ , the warped signal is obtained:

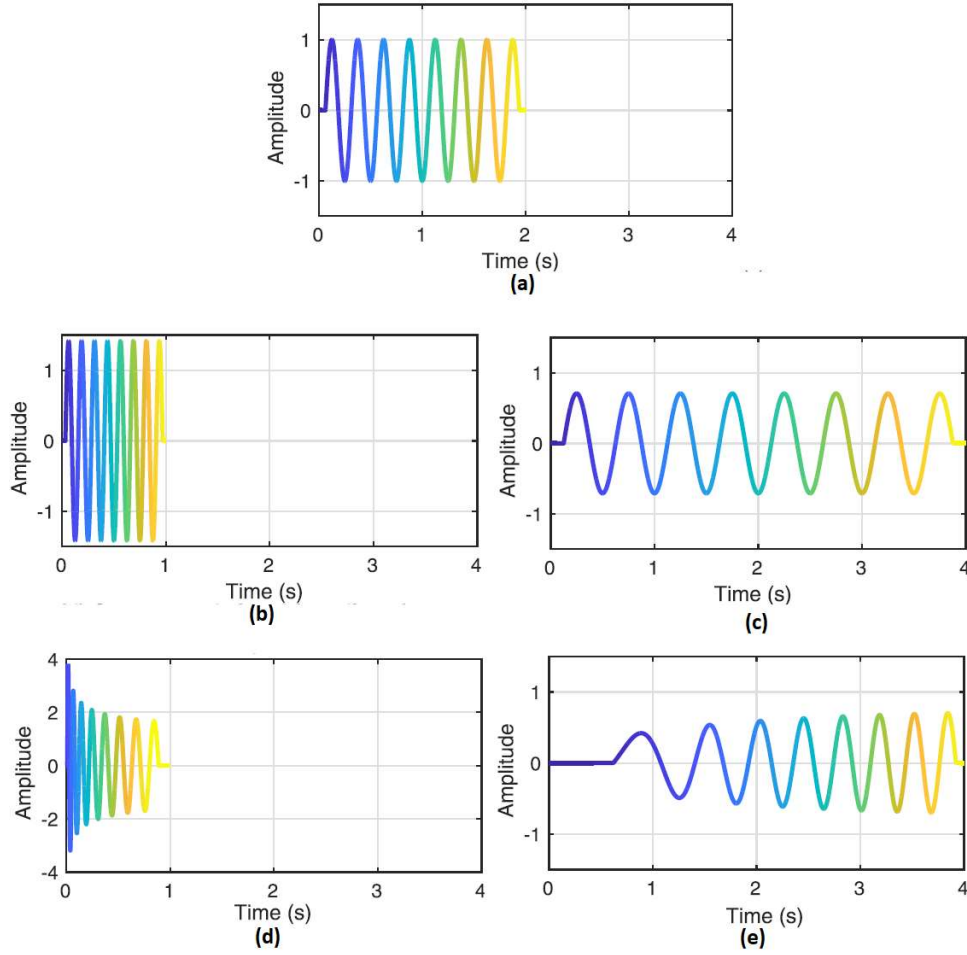


Figure 3.11: Comparison between linear and non-linear time warping methods [18].

- (a): Original signal.  
 (b): Linear compression. (c): Linear stretching.  
 (d): Non-linear compression. (e): Non-linear stretching.

$$y_w(t) = \sqrt{|h'(t)|}a[h(t)]e^{-i2\pi f_0 t} \quad (3-20)$$

The above equation shows that the warped signal has a linear phase  $\Phi(t) = t$ . It is worth mentioning that phase function is unknown in real-life applications and it should be estimated through modal propagation in the medium (see chapter 5).

### **3.6 Summary:**

This chapter started with LTI systems and Fourier transform. Different types of signal representation based on Gabor transform or wavelet transform are described. Dynamic mode decomposition and warping techniques that are required to discriminate modes for modal filtering were explained in detail.



## CHAPTER 4

### Literature Review

This chapter reviews previous efforts in acoustic underwater localization, mainly focusing on signal processing approaches. The State-of-the-art techniques for acoustic localization can broadly be divided into two main groups: data-driven methods and model-based methods (Figure 4.1.). Data-driven approaches learn directly from data. In other words, these methods only rely on acoustic data and do not need any information about the waveguide to predict the location of the sound source. On the other hand, model-based methods should mathematically model the environment and its effects on the travelling signals. In the following, more details of each group will be presented.

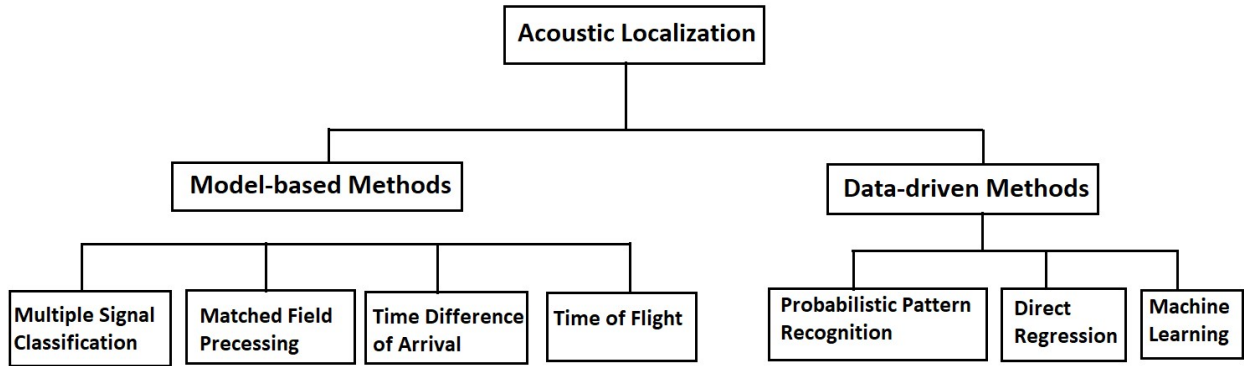


Figure 4.1: Overview of the acoustic localization techniques.

#### 4.1. Data-driven Methods

Data-driven approaches aim to automatically extract implicit information from the collected data. The obtained knowledge can be used later for various tasks. Take source localization as an example; based on the known location of the sound source and recorded acoustic data by the hydrophones, a position is assigned to each data. This set of collected data with predefined labels is called training set.

Since there is a positive correlation between accuracy of the data-driven methods and quality of the collected data, the process of training set preparation becomes important. It is believed that accuracy and reliability of these methods are proportional to quantity and quality of the training set. It should be noted that training data collection is a laborious and time-consuming task. In a

dynamic environment like ocean, for example, different factors such as pressure, salinity, and temperature of water affect the speed of sound [30]. So, data at various depths should be recorded to cover the whole gamut of water pressure and temperature.

Data-driven methods have several shortcomings. Firstly, these methods do not have generalization capability. The collected data for one environment cannot be used for another environment, which means the data collection process should be repeated for the new situation. For instance, sound signals collected for localization in a confined tank cannot be utilized for an open space underwater. Secondly, these methods are complex and have a black-box nature. Therefore, it is difficult to interpret these methods to acquire physical insights.

Data-driven methods are either supervised or unsupervised [31]. In supervised learning, the goal is to learn a predictive mapping from inputs to outputs using training set with known labels. In unsupervised learning, however, no labels are available, and the task is to extract complex and subtle patterns within the data.

#### **4.1.1. Machine Learning**

Most of the machine learning techniques are supervised learning. They are aimed at finding a mapping from inputs to outputs according to their training set. Take acoustic localization into consideration; the input is the received sound signal, captured by the hydrophone and the output is the position of the sound source. Various machine learning methods have been deployed for localization, ranging from simple methods such as nearest-neighbor classifiers and Support Vector Machine (SVM) to more sophisticated algorithms like Deep Neural Network (DNN) [31].

A machine learning-based method has been proposed for auto-detection and localization of targets in underwater acoustic array networks [32]. Fractional Fourier Transform (FrFT) was used to find the peak of the reflected linear frequency modulated (LFM) signals emitted by a sensor array. Based on the location of the peak, the target distance and radial velocity were estimated.

In [33], AUV-aided localization for Internet of Underwater Things (IoUT) was used by a reinforcement-learning (RL). The hybrid network architecture consists of surface buoys, autonomous underwater vehicle (AUV), and active and passive sensor nodes. Two neural

networks were adopted to approximate the increment policy and value function in the RL-based localization algorithm, and minimize the sum of all measurement errors.

Three conventional machine learning techniques, feed-forward neural networks, support vector machines, and random forests (RF) were trained by the received pressure collected from a vertical linear array to estimate source ranges in an ocean waveguide [34]. These machine learning techniques have also been used for acoustic localization in a confined test tank [35]. Furthermore, a Convolutional Neural Network (CNN) was trained by the spectrogram images of the received signals.

Energy consumption of active sonar localization methods depends on the two-way travel time of underwater acoustic signal. Reinforcement learning was employed to improve the accuracy and energy efficiency of such system by optimizing the beacon selection policy without relying on the channel model between the beacon and the target [36].

Deep convolutional denoising autoencoder was used for moving targets detection and tracking. Reflections of an active acoustic emitter were used for training the neural network in order to minimize power resources in offshore monitoring platforms [37]. In [38], DNN was proposed for localizing unknown nodes in underwater wireless sensor networks (USWNs), and its performance was compared with SVM, and generalized least squares (GLS) in terms of localization accuracy and efficiency.

#### **4.1.2. Direct Regression**

Since the output space is continuous and structured in the source localization application, regression methods have also been used for this purpose. Regression analysis aims to discover the relationships between the outcome variable and independent variables, called features. In the case of sound localization, for example, the outcome variable is the position of the sound signal, and the features are received sound signals.

The potential of regression methods for underwater source localization in fluctuating ocean was studied in [39]. Two regression models, a kernel regression, and a piecewise linear regression, have been used for this purpose. Train and test data sets had been collected in tank conditions and they used to reproduce fluctuating environments in closed and well-mastered settings.

In [40], source localization is regarded as a supervised learning regression problem, and it was solved by generalized regression neural network (GRNN). By using several snapshots, the normalized sample covariance matrix (SCM) was formed and used as the input of the GRNN. After training the neural network, the source position was estimated directly from the normalized SCM with GRNN.

Performance of regression and classification neural networks for single-source direction-of-arrival estimation was compared in [41]. The output space was described based either on the angular distance between spherical coordinates or on the mean squared error between Cartesian coordinates. It was shown that regression on Cartesian coordinates is generally more accurate, except when localized interference is present.

SVM can also be used for regression. The regression version of SVM, called support vector regression (SVR), was utilized for head-related transfer functions (HRTFs) based sound source localization [42]. A virtual listener based on SVR was proposed to substitute the human listener, and it was trained by a small training set, obtained by sampling uniformly a subject's HRTFs across directions. Experimental results showed that the virtual listener achieves human-level localization accuracy.

Unknown physical parameters of the acoustic environment were estimated by Gaussian process regression (GPR) and used for acoustic source localization in an acoustic sensor network (ASN) [43]. The estimated distance is then used by an ASN with known relative node positions for acoustic source localization. A sparse Gaussian process regression was deployed to adjust the amount of shared data between the sensor nodes to meet the network constraints.

#### **4.1.3. Probabilistic Pattern Recognition**

Unlike conventional pattern recognition methods that only give the most likely class for the given input, a probabilistic classifier provides the probability distribution over a set of classes.

To tackle weaknesses of the sonar image such as speckle noises and low-resolution images, a probability-based framework was proposed in [44] to recognize consecutive sonar images. Particle filtering and Bayesian feature estimation were used to repeatedly estimate the continuity

and feature of objects in sequential images. These probability methods enabled the system to repeatedly predict and update the status of the object of interest by a stochastic method.

In [45], two probabilistic neighborhood-based data collection algorithms were proposed to acquire marine environment information using three-dimensional underwater acoustic sensor networks (3D UASNs). They used probabilistic acoustic communication model instead of the traditional deterministic acoustic communication model to compensate decreased successful information delivery probability.

A probabilistic neighborhood location-point covering set-based data collection algorithm was proposed for UASNs [46]. To optimize the data collection latency, the proposed algorithm initially generates a space lattice set to establish the probabilistic neighborhood location-point covering set for data collection. Then, an autonomous underwater vehicle traverses only location points in the constructed covering set with a hierarchical grid-based obstacle avoidance strategy.

In [47], Bayesian process was used to obtain probabilistic direction estimation for source localization using multiple underwater acoustic sources. First, target acoustic signals were extracted and identified based on frequency bands of each source. Then, time difference of arrival of two hydrophones was utilized to localize the underwater acoustic sources. Finally, the direction angles acquired from various locations of the vehicle were used to perform extended Kalman filter based localization of underwater acoustic sources.

Underwater localization using wireless acoustic communication signals was performed by probabilistic pattern recognition in eigenspace of principal components analyses (PCA) [48]. The scheme was based on fingerprinting and included training and predicting stages. It was assumed that if the projected features have Gaussian probabilistic distributions, probabilistic pattern recognition of projected features in PCA space can be used for localization.

#### **4.2.Model-Based Methods**

Localization can be regarded as the estimation process that concerns with the sound source coordinates. Estimation methods can be divided into parametric and nonparametric classes. *Nonparametric* estimation is aimed at finding the value of the estimate, without considering probability distributions parameters such the mean and variance. A good illustration for

nonparametric estimator is bearing estimation using a line array. On the other hand, *parametric* estimator assumes a probability distribution with fixed set of parameters that generates sample data. The goal of parametric estimator is to find these parameters of the signal or parameters describing the medium. It is worth mentioning that most well-known localization methods are parametric. Inverse problem is one of the parametric methods that aims at extracting some information of the medium (such as ocean sound speed, density) from the received signal. After estimating the medium property and determining sound propagation mechanism in it, acoustic ranging can be performed through the following methods.

#### **4.2.1. Time Difference of Arrival (TDOA)**

Time difference of arrival is based on the time of arrival (TOA), the time difference between transmission and reception of a sound signal. For accurate measurement, sound source and receiver should be synchronized with each other to be aware of the exact starting time of the sound generation [50]. TOA measurement also requires distance-related information between a source and receivers which can be obtained by the inverse problem approach.

Being time-synchronized with the source, the receiver calculates the delay upon receiving the acoustic signal. Then, the range is estimated by multiplying the sound speed in the medium by the TOA. The range estimation results in a circular locus of possible source positions with the receiver at the center. To pinpoint the location of the source in a 2D space, at least three receivers are required; the position of the source is at the intersection of three circular locus.

Cross correlation between received and reference signals was used to measure TOA for localization inside a confined test tank, using an array of 4 hydrophones [51]. To improve the TOA estimation and consequently precision of the localization system, pseudo-random binary sequences modulated in Binary Phase Shift Keying (BPSK) was proposed [52].

Synchronization error between sound source and receiver brings about ranging inaccuracy. To mitigate this error, time difference of arrival method has been proposed [50] which is based on pairs of spatially separated hydrophones. One of hydrophones is considered as the master (reference), while the remaining are the slaves (auxiliary). Only time synchronization between auxiliary sensors is needed in this method. In the 2D case, the possible location of a source for

each TDOA is given by a hyperbolic line of position in which the focal points of the hyperbola are the positions of the two receivers used in the TDOA computation.

Cross-correlation is one of the most common methods to measure TDOA [53]. Multiple surface beacons have been used to obviate the need for time synchronization between the surface beacons and underwater source [54]. The underwater node receives the positioning messages from surface beacons belonging to the same grid and calculates its location by itself using these messages and the corresponding arrival times. Modified versions of TDOA localization method were presented to address the problem of variable received positioning messages at one epoch.

To improve estimation bias and accuracy, TDOA method was combined with bearing-angle-of-arrival (BAOA) measurement that shows the direction from which the signal is received. To increase the accuracy in the presence of large noise, an iterative constrained weighted least-squares method was presented in the TDOA/BAOA method [55].

#### **4.2.2. Time of Flight (TOF)**

To have asynchronized sound transmitter and the receiver, TOF method has been proposed. However, in TOF method, nodes should be able to send and receive acoustic signals simultaneously. First, the transmitter emits a sound signal. Upon receiving this signal, the receiver sends another sound signal in response. Finally, the transmitter calculates the distance according to the round-trip-time [51].

Time of flight and received signal strength (RSS) measurements were combined for underwater acoustic sensor network (UASN) localization in inhomogeneous underwater medium [56]. First, transmission loss for acoustic wave propagation was measured. Then, an oversampled matched filter-based method for RSS measurement was proposed in asynchronous transmitter–receiver scenario. Finally, an iterative localization algorithm was obtained. The authors improved their method [57] by developing an Array-RSS localization method based on an iterative algorithm using the RSS parameter of the beamformer output.

#### **4.2.3. Matched Field Processing**

Match field processing (MFP) aims to find range and depth of the sound source when the propagation model, source frequency, ocean depth, and seabed characteristics are known. It

should be noted that if the model parameters are inaccurate, viable and precise solution cannot be obtained. To estimate the location of the sound source, the vertical hydrophone array provides a vector of measurements of the true field. Then, the model estimates these measurements for a given set of source coordinates. By finding the maximum of the magnitude squared of the normalized inner product of true and estimated vectors, the solution can be obtained [49]. In other words, MFP matches received array data to a dictionary of replica vectors for source localization.

Since number of replicas far exceeds the number of sources, the solution set is sparse. To cope with sparsity problem, the matched field problem was reformulated as an underdetermined, convex optimization problem [58]. Compressive sensing (CS) uses a row-sparsity constraint to estimate the optimum unknown source amplitudes using the replica dictionary.

Mismatching between the received acoustic field and its model and its effect on source localization was considered in [59]. Different approaches to increase the stability of the algorithms for source position estimation were also reviewed [59].

Performance of conventional MFP for underwater acoustic source localization has been improved by utilizing multiple arrays [60]. It was assumed that relative calibration between arrays is known, so further information was captured from variation in received signal amplitude between arrays. More information extracted from phase variations also incorporated into conventional MFP when arrays were synchronized.

#### **4.2.4. Multiple Signal Classification**

Multiple signal classification (MUSIC) is an algorithm for parameters estimation from recorded signal measurements. This method provides high-resolution signal estimation by isolating signal and noise subspaces. Signal can be separated from noise because the algorithm assumes that the number of components is known in advance. Although some efforts have been done to estimate the number of components from autocorrelation matrix of the signal, previous knowledge about the number of components curtails MUSIC algorithm application.

MUSIC was implemented on an autonomous underwater vehicle in [61]. An array of four pre-calibrated hydrophones was utilized for geometry-dependent MUSIC computation, which



improved acoustic localization accuracy. A modified version of the algorithm, called normal-mode based MUSIC, was introduced to make DOA estimation in shallow water less biased [62].

Performance of the conventional MUSIC under an extremely low SNR environment was enhanced by assimilating Jordon canonical matrix in the covariance matrix for the reconstruction of data [63].

In [64], MUSIC algorithm was proposed for locating small inclusions buried in a half-space, using the far-field theory. The locating method was based on measuring the scattering amplitude at a fixed frequency. Another variant of MUSIC, called mixed polarization MUSIC (MP-MUSIC) algorithm, was proposed in [65] and signal polarization was taken into consideration. MP-MUSIC is suitable for underwater localization as it provides space position with low computational time.

#### **4.3.Summary:**

This chapter reviewed state-of-the-art underwater source localization methods. Both data-driven and model-based methods were covered in this chapter.

## CHAPTER 5

### Dispersion-based Acoustic Source Localization

In this chapter, a signal processing based acoustic underwater localization method will be presented. It should be noted that this method relies only on one hydrophone, and adopts warping approach as a non-linear signal processing method to make modals in the received sound signal more separable. After converting the sound signal into time-frequency domain and applying warping, modes are filtered. By comparing the estimated modal dispersion curve from the received signal and the one obtained from the environmental model, the location of the sound source can be estimated through an iterative optimization method.

#### 5.1 Discrete Warping

Chapter 3 described warping theory to linearize the signal phase. Warped modes with linear phases can be more easily separated. To implement warping with a computer, however, discrete version of warping should be implemented.

Assume a continuous signal  $y(t)$  in  $[t_{min}, t_{max}]$  interval. The discrete version of the signal,  $y[k]$ , can be obtained by sampling at a frequency of  $f_s$ . According to the Nyquist rate theory [66], to have a distortion-free discrete signal, sampling frequency should be twice the highest frequency of the signal. Denoting the warping function with  $h(t)$ , sampling frequency of the warped signal is:

$$f_s^h = \frac{2f_s}{\frac{t_{max}}{h^{-1}(t_{max})}} \quad (5-1)$$

where  $h^{-1}$  is the inverse warping function. The discrete version of the warped signal is:

$$y_w[k] = \sqrt{\frac{\bar{t}_k}{h(\bar{t}_k)}} y[h(\bar{t}_k)] \quad (5-2)$$

where  $\bar{t}_k = \frac{k}{f_s^h}$  and  $h(\bar{t}_k) = (\bar{t}_k^2 + t_r^2)^{0.5}$ .  $t_r$  is the travel time of the fastest mode which equals to  $t_r = \frac{r}{C_w}$ , where  $r$  is the distance between sound source and receiver, and  $C_w$  is the speed of sound in the water.

The discrete version of the unwarping signal is obtained by inverse warping as follows:

$$y_u[n] = \sqrt{\frac{t_n}{h^{-1}(t_n)}} y_w[h^{-1}(t_n)] \quad (5-3)$$

with  $t_n = t_{min} + \frac{n}{f_s}$ ,  $h^{-1}(t_n) = (t_n^2 - t_r^2)^{0.5}$ .

Assume an ideal waveguide with perfectly reflecting seabed and sea surface in which sound speed is constant in water. The received signal phase is proportional to  $\Phi(t) \propto \sqrt{t^2 - t_r^2}$  [67]. It is obvious that for this phase function, the warping function would be  $h(t) = \sqrt{t^2 + t_r^2}$ . One can see that for finding the appropriate warping function,  $t_r$  is required. Since  $t_r = \frac{r}{c_w}$ , the exact values of range (sound source/receiver distance) and water sound speed should be known. However, the range parameter is the parameter of interest and it is unknown. Fortunately, the warping algorithm is not very sensitive to these parameters, so one can choose typical values for range and sound speed to obtain relatively accurate results. Figure 5.1 shows sensitivity of the warping algorithm to these parameters. A sinusoidal wave was warped with  $r = 10km$ ,  $c_w = 1500m/s$ . The signal is then unwrapped with different parameters.

For the next experiment let us assume that the true value of the range was  $r = 10km$  but we set  $r = 15km$  as the initial value. As figure 5.2 shows, although warping signals are different for different ranges (figure 5.2 (b)), unwarping signals are almost identical (figure 5.2 (a)). Therefore, it is not necessary to know the exact value of the range to use warping, and a rough estimation would be enough.

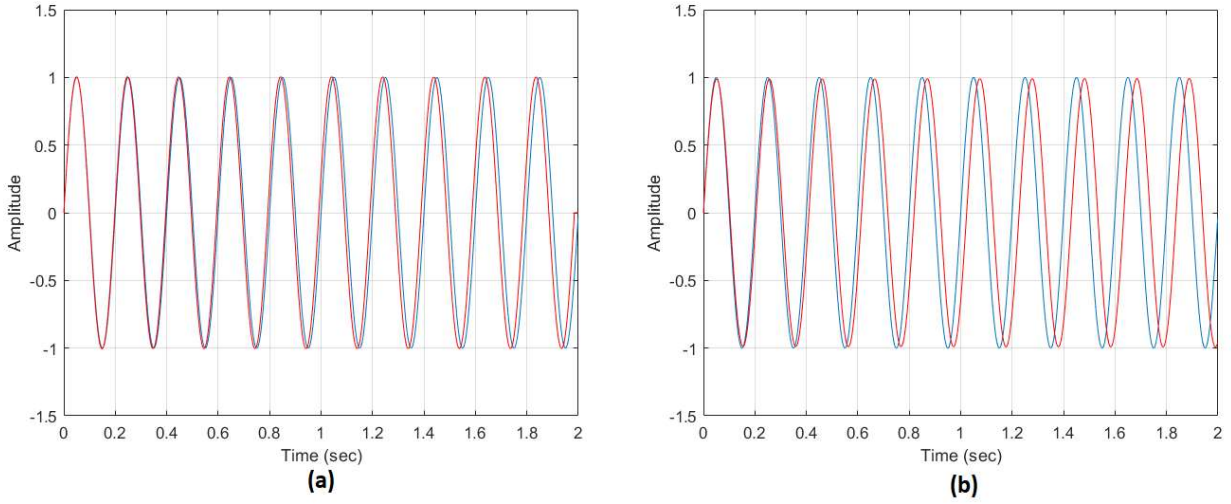


Figure 5.1: Sensitivity of warping and unwarping algorithms to range and sound speed parameters.  
 (a): Original signal and signal after warping with  $r = 10km$  and unwarping with  $r = 11km$ .  
 (b): Original signal and signal after warping with  $c_w = 1500m/s$  and unwarping with  $c_w = 1600m/s$ .

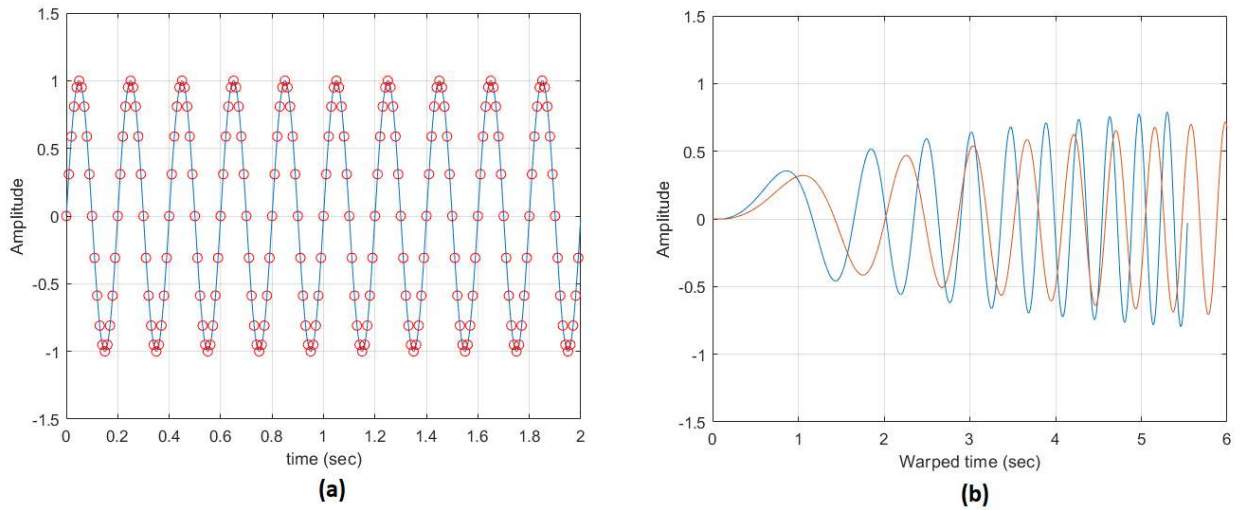


Figure 5.2: Sensitivity of warping algorithm to range parameter.  
 (a): Unwarping signals with  $r = 10km$  and  $r = 15km$ .  
 (b): Warping signals with  $r = 10km$  and  $r = 15km$ .

## 5.2. Impulse Signal Warping

The warping function should be able to work with different signals. Among them, impulse signal plays a pivotal role in system identification as systems are generally described by their impulse response, the system output when an impulse signal is presented as its input signal. As stated in Chapter 2, the output of a linear time-invariant (LTI) system to any input is a function of the input and the impulse response. From mathematical point of view, an ideal impulse function is a

function that is zero everywhere but at the origin, where it is infinitely high. However, producing an ideal impulse signal is not possible in practical applications. Therefore, a pulse that is short enough compared to the impulse response is regarded as an impulse signal. Figure 5.3 shows a train of impulse signal, including 10 impulsive signals. A good illustration of the train of impulse signals is AUV localization in which the AUV generates beep sounds repeatedly.

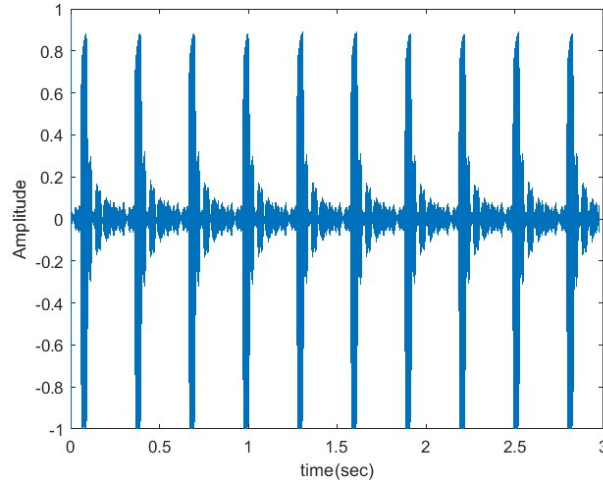


Figure 5.3: A train of impulse signal.

Since an impulse signal has a short time duration, selecting the time origin, the arrival of the fastest mode, becomes more important. Assume a noisy underwater environment with sound speed of  $c_w$  in water and  $c_b$  in seabed. If the distance between sound source and receiver be  $r$ , the first signal arrives at  $t = \frac{r}{c_w}$  to the hydrophone. However, the sound arrives sooner to the hydrophone from seabed medium since  $c_b > c_w$ . This signal is highly attenuated which makes it difficult to be differentiated from the noise. Figure.5.4 shows the impulse response of the environment. Different time origins corresponding to the true starting values are shown with vertical lines between 6s and 7s. Early time origin, accurate time origin, and late time origin are indicated in figure 5.4 with (a), (b), (c), respectively. The spectrograms of the warping signals with different time origins are depicted in figure.5.5.

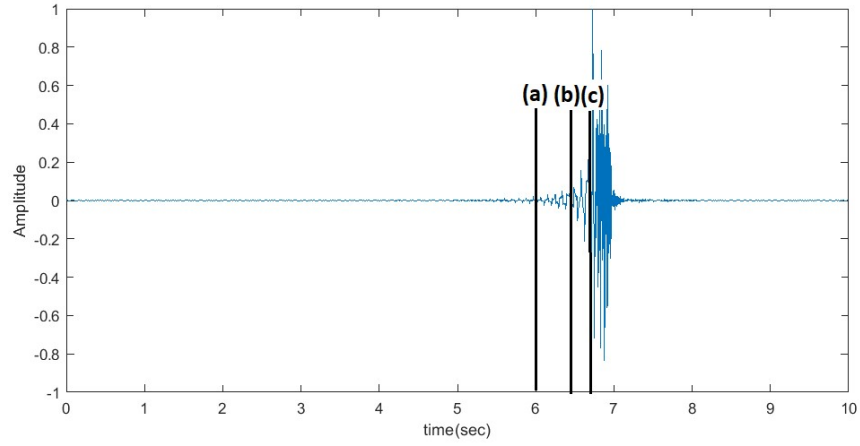


Figure 5.4: Uncertainty in the time origin.

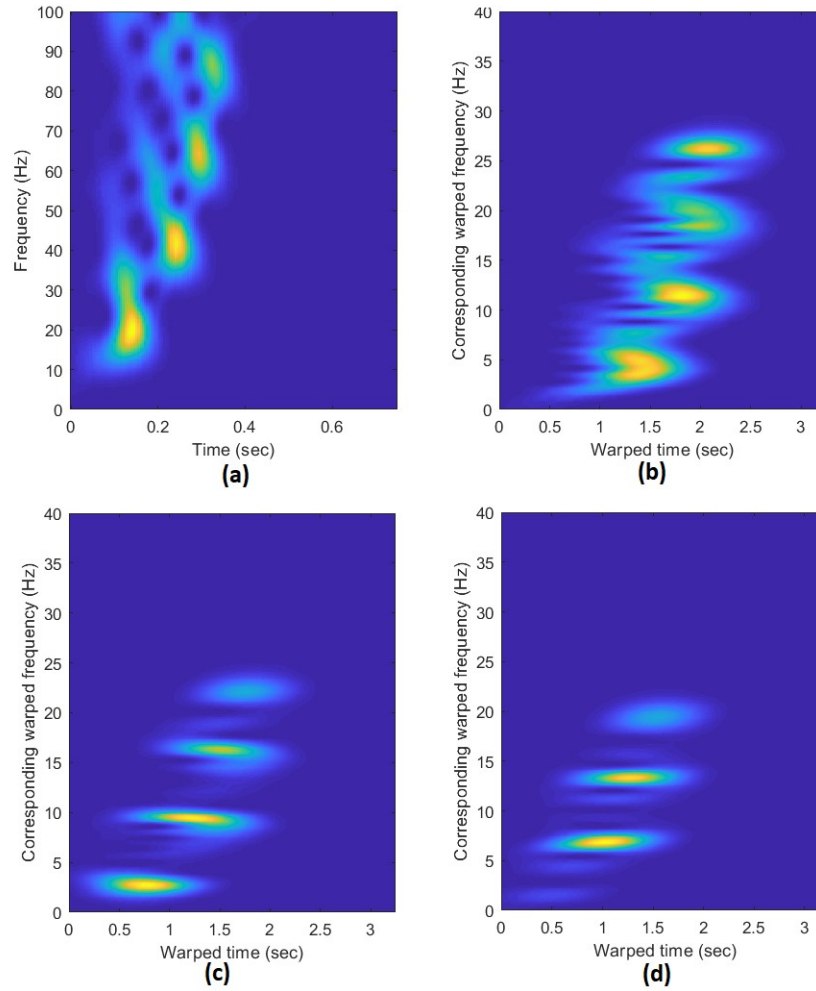


Figure 5.5: Spectrograms of different warping signals.

(a): Overall signal. (b): Signal with early time origin.

(c): Signal with accurate time origin. (d): with late time origin.

According to figure 5.5 (b), although early time origin results to four horizontal warped modes, the modes are not perfectly separable. The accurate time origin brought about four separable modes with minimum overlaps (figure 5.5 (c)). Modes are also completely distinguishable in figure 5.5 (d), but the first mode was missed. It is obvious that time origin setting is important, and this process should be performed in a manner to maximize modal separability without losing the fast mode.

### 5.3 Known Signal Warping

Most of the natural sound signals are not impulsive. For general acoustic sound signals localization other preprocessing steps should be performed to improve the warping performance. If the Fourier transform of the signal,  $s(f)$ , is known, we can use this information to counteract the effect of frequency variations due to the source signal. This process is called *deconvolution* and it can be performed by dividing the environmental filtering effect (Equation 2.2) by  $s(f)$ . Figure. 5.6 (a) shows a modulated FM signal in time domain which its frequency decreases over time. Spectrogram of this signal is shown in figure. 5.6 (b). Figure 5.6 (c) and (d) depict time domain and spectrogram of the signal after being affected by the environment.

As it is obvious in figure 4.6 (d), modes are very convoluted, and it is not easy to segregate them. However, by source deconvolution, one can easily separate the modes (figure. 4.7 (b)). This technique is useful when some knowledge about the sound source is available. For instance, we know about the sound signal of a ship in advance, and this information can be used for the received signal deconvolution.

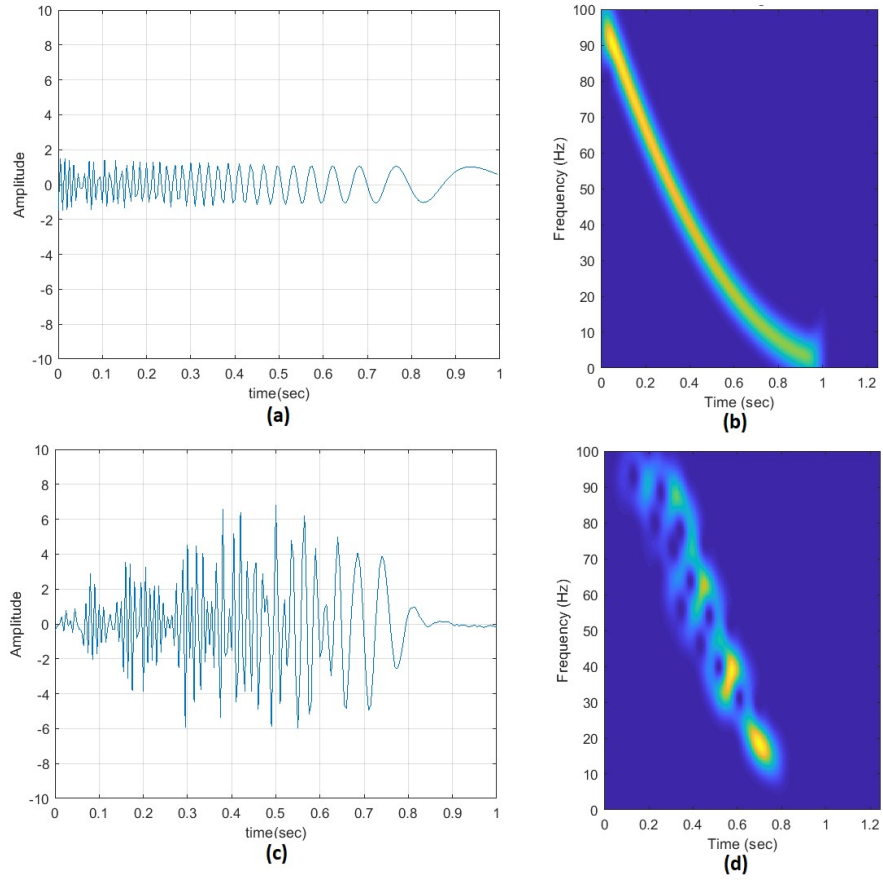


Figure 5.6: Spectrograms of different warping signals.

(a): Overall signal. (b): Signal with early time origin.  
(c): Signal with accurate time origin. (d): with late time origin.

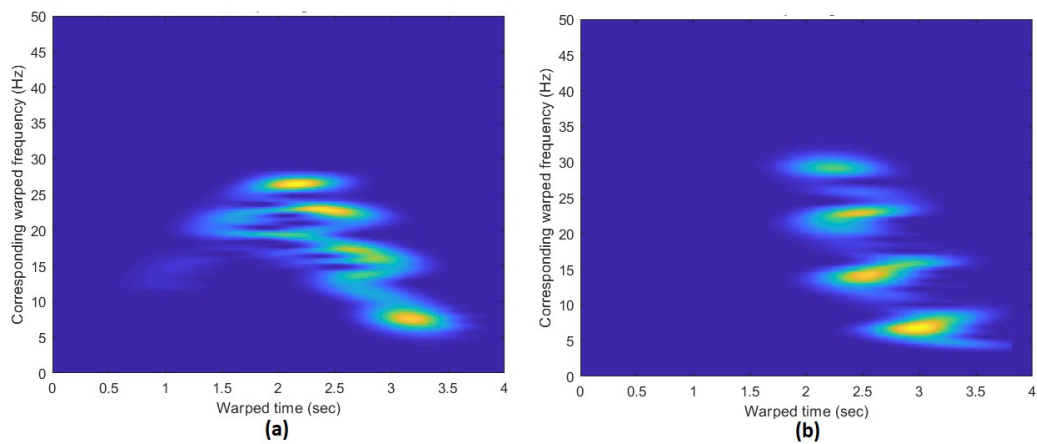


Figure 5.7: Effect of source deconvolution on warping.

(a): Signal warping without deconvolution. (b): Signal warping with deconvolution.



## 5.4 Unknown Signal Warping

In most of the real-life scenarios, signal deconvolution is not applicable as accurate knowledge about the source signal is not available. A good illustration is underwater mammal localization which their acoustic signals vary from one type to another one. When it comes to unknown signals, we can modify the phase of the received signal based on the estimation of the source signal phase:

$$y_c(f) = y(f)e^{-i\Phi_s(f)} \quad (5-4)$$

The above equation is called *phase compensation*. The compensated signal ( $y_c(f)$ ) is obtained by multiplying the original received signal ( $y(f)$ ) by the estimated phase of the source signal ( $\Phi_s(f)$ ). Warping will be performed on the compensated signal. To estimate the  $\Phi_s(f)$ , the arrival of the first mode, which is less affected by dispersion, can be manually selected.

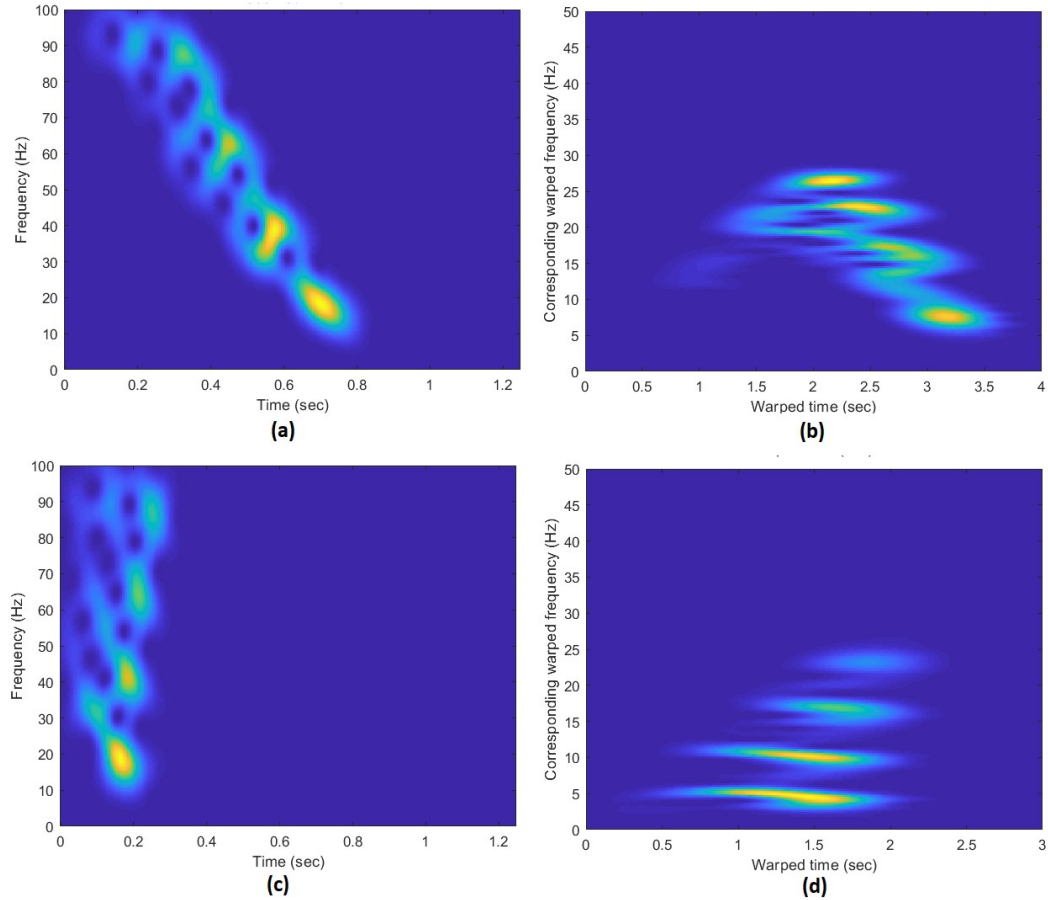


Figure 5.8: Effect of phase compensation on warping.

(a): Original signal. (b): Warping the original signal. (c): Compensated signal. (d): Warping the Compensated signal.

Comparing the warped signals in figure 5.8 (a) and (b), one can see that modes are separable after phase compensation. The phase compensation technique is not very sensitive to the phase estimation. As figure 5.9 shows, modes can be separated under different phase estimations. Therefore, warping is an effective method even when little information is available about the source.

#### 4.4. Modal Filtering

As stated before, due to dispersion, a signal hydrophone receives several distinct arrivals components, called modals. Modal filtering aims to extract individual modes from the received signal, and it is a critical preprocessing step in the acoustic localization. After extracting one mode, it can be used to estimate the location of a sound source by comparing relative arrival time and amplitude of the mode with the corresponding parameters of a hypothetical mode generated by the propagation model of the underwater environment.

To have an efficient filtering, warping technique is deployed to separate the modes by converting them into horizontal lines in the TF domain. For this purpose, prior information about the sound source should be leveraged to perform preprocessing steps such as time origin selection, signal deconvolution, and phase compensation, which bring about better modal separation.

After warping the received signal, a *mask* should be defined to indicate which mode should be extracted from the spectrogram of the signal. Working in the TF domain, the mask is a 2D area which defines the region of interest. While value of 1 is assigned to the region under the mask, other TF regions are set to 0. Figure 5.10 shows the received signal and the mask for filtering the second mode.

It should be noted that the mask is applied on the Short Time Fourier Transform (STFT) of the signal and not on its spectrogram.

$$M(f, t) = F(f, t)S(f, t) \quad (5-4)$$

where  $F(f, t)$  is filter,  $S(f, t)$  shows the signal, and  $M(f, t)$  is the selected mode. Figure 5.11 depicts different modes extracted by the filtering process.

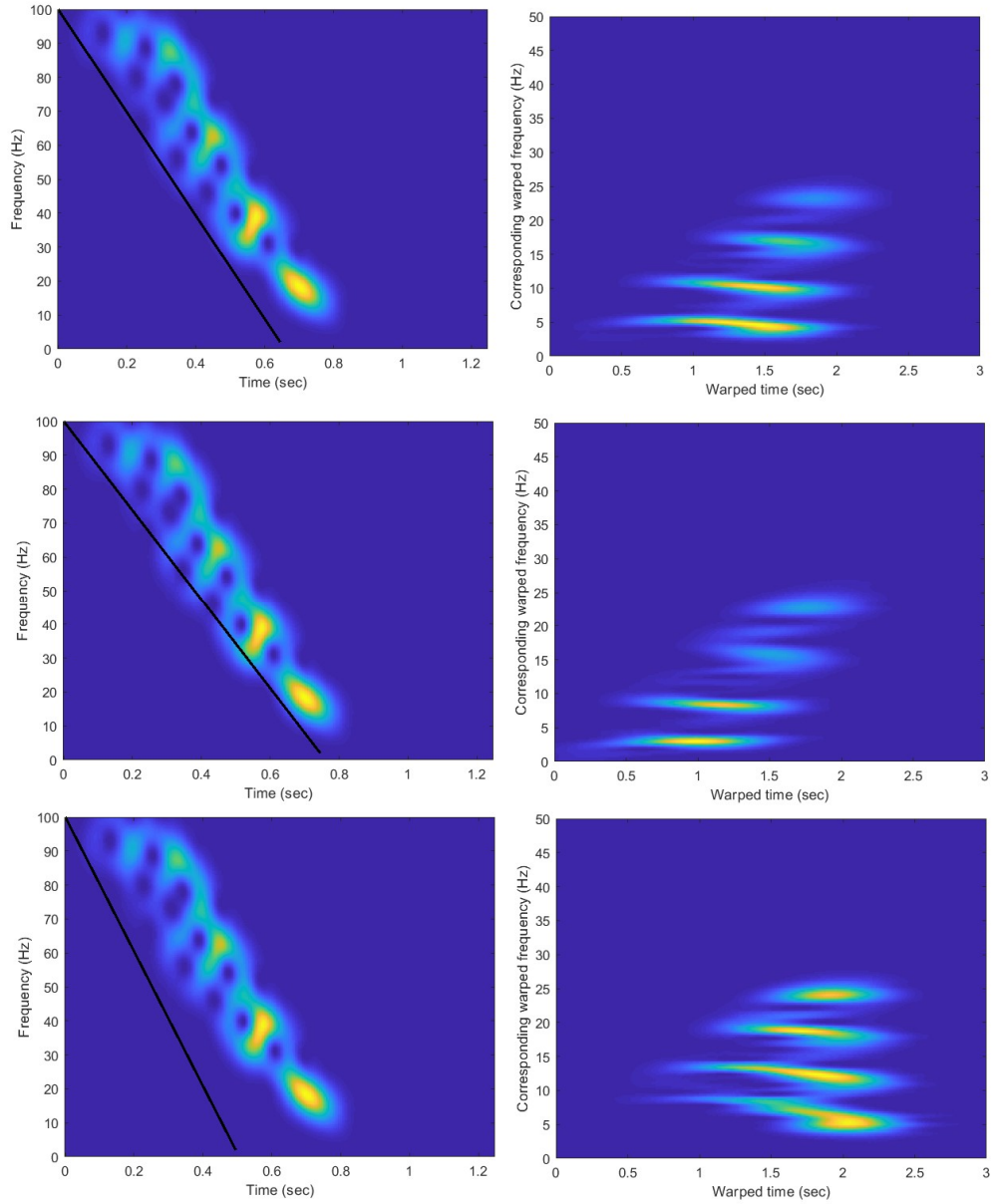


Figure 5.9: Warping robustness to the source signal phase estimation.  
 Left column: Received signal and different phase estimations, shown with a solid line.  
 Right column: Corresponding warped signals.

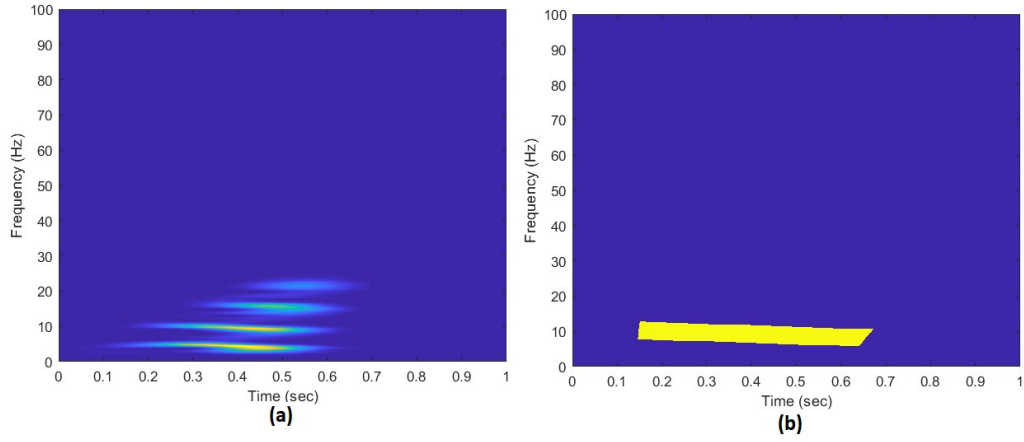


Figure 5.10: Filtering mask.  
(a): Received signal. (b): Second mode selecting mask.

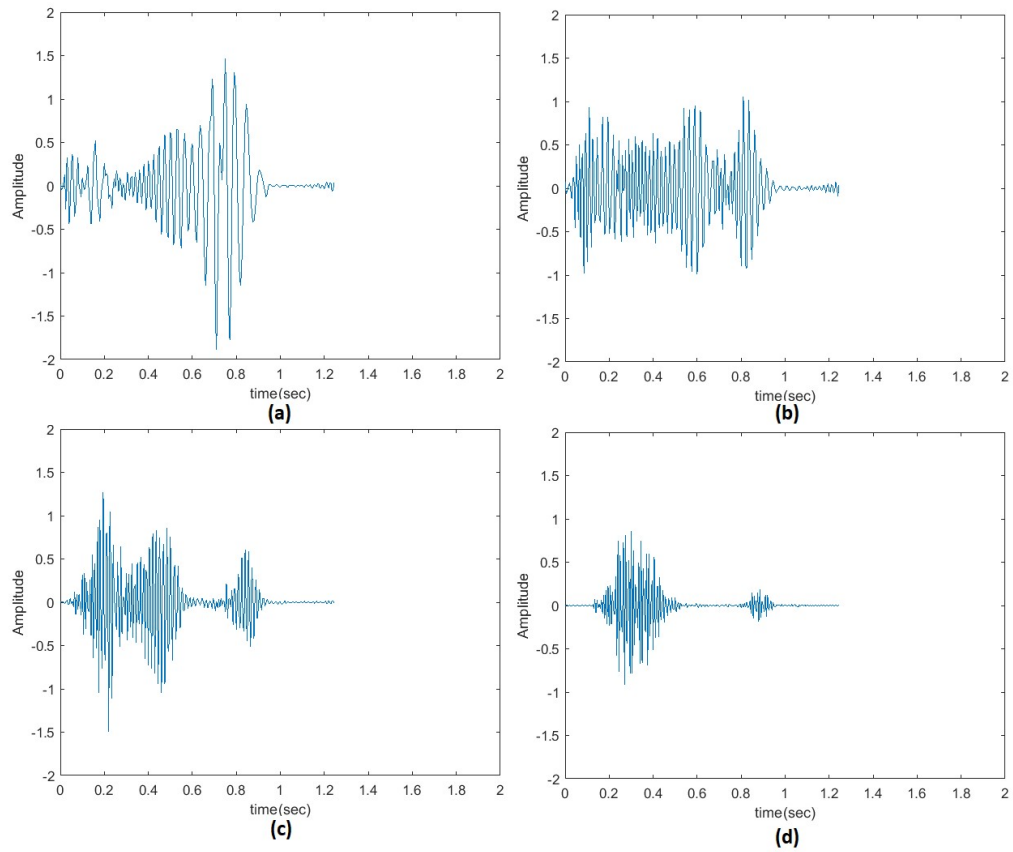


Figure 5.11: Filtering process.  
(a): First mode. (b): Second mode. (c): Third mode. (d): fourth mode.

## 5.6 Dispersion curve estimation

As mentioned in chapter 2, the TF position of a given mode is called the *dispersion curve*, and it is obtained by equation 2.4. According to this equation, the modal travel time depends on the distance between sound source/receiver and modal group speed. An approximate closed-form expression for dispersion curves can be obtained from the modal propagation equation [24]. Instead of analytical methods, numerical simulations can be used to find dispersion curves [11]. Figure 5.12 shows the dispersion curves obtained from the Pekeris waveguide. Each dispersion curve has a specific point where the curve bends sharply. This point is called the Airy phase and indicates the last modal arrival. Consider the second mode in figure 5.12, the Airy phase is about 40Hz. Signals with lower frequency than the Airy phase propagate through the seabed and arrive faster. Since the seabed attenuates these signals, they are not usually visible in real applications.

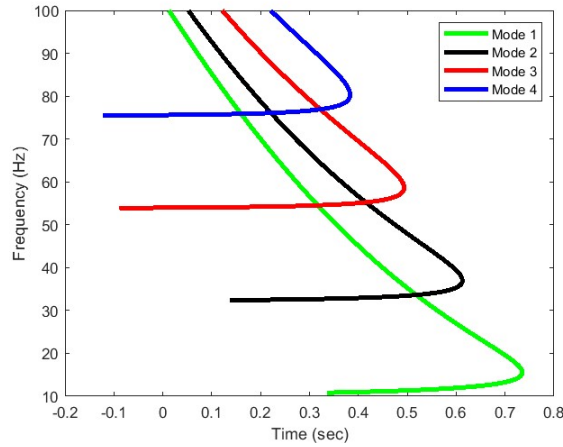


Figure 5.12: Theoretical dispersion curves of the first four modes.

To verify the accuracy of the propagation model, the dispersion curves are superimposed to the spectrogram of the received signal. Figure 5.13 shows that dispersion curve of each mode matches with the location of the corresponding mode in the TF domain.

After filtering one mode which is a mono-component signal, the group delay of the extracted mode (equation 2-4) can be measured from the first order moment [68]:

$$t_m(f) = \frac{1}{E} \int_{-\infty}^{+\infty} t \times tfr(t, f) dt \quad (5-5)$$

where  $E$  is the energy of the signal and  $tfr(t, f)$  is the time-frequency representation of the signal. It is worth mentioning that the first order moment represents the average arrival time of the spectrogram of the filtered mode.

Figure 5.14 compares theoretical dispersion curve obtained by modal propagation and estimated dispersion curve obtained by warping technique. As it can be seen, theoretical and estimated dispersion curves are well-matched over mode frequency range. For example, for the first mode, the two curves completely overlap each other in the interval of 15Hz to 50Hz (figure 5.14 (a)). However, between 50Hz and 80Hz, the two dispersion curves are a little bite mismatched. The error stems from the interference between modes which could not be rejected completely by the filter. One can see that theoretical and estimated dispersion curves are completely different at below Airy phase frequencies. This is due to the fact that propagation through seabed is not modeled in the warping. For more accurate localization, dispersion curves should be restricted to the frequency band of interest (figure 5.15).

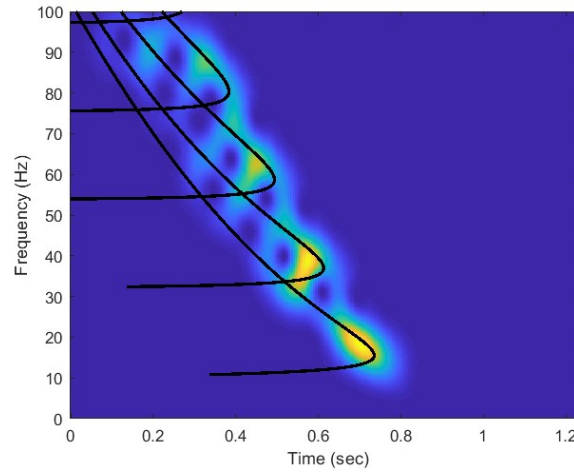


Figure 5.13: Estimated dispersion curves of the first four modes.

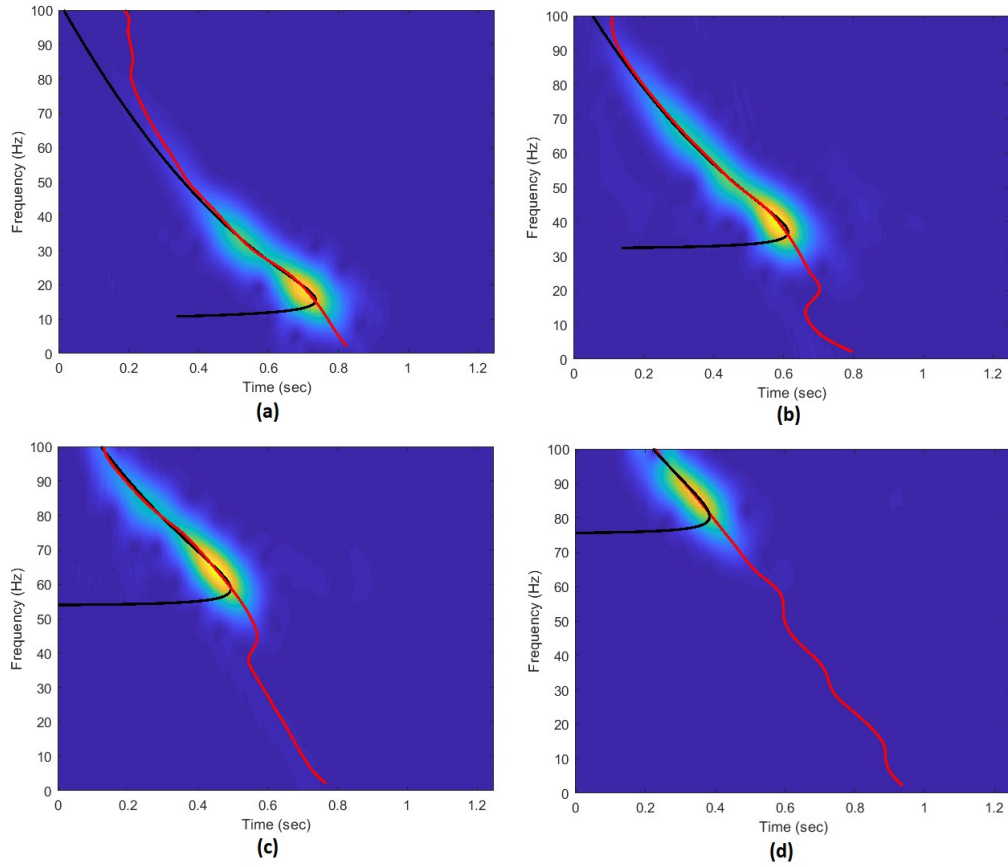


Figure 5.14: Comparison between theoretical and estimated dispersion curves.  
(a): First mode. (b): Second mode. (c): Third mode. (d): fourth mode.

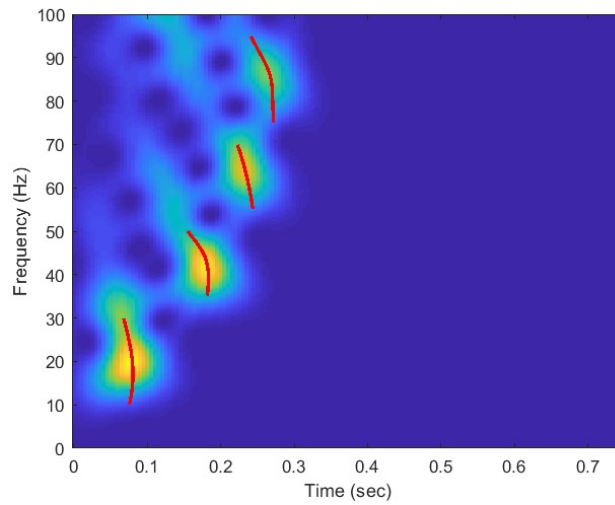


Figure 5.15: Modal dispersion curve restriction.

## 5.7 Rang Estimation

Range estimation aims to find the optimum value of the distance between sound source and receiver. After estimating modal dispersion curves, this information can be used to estimate the location of the sound source. To this end, *theoretical* dispersion curves (obtained from Pekeris model) and *estimated* dispersion curves (acquired from average arrival time of the mode) will be compared with each other. We will use an iterative approach to match theoretical and estimated dispersion curves over different parameters. The best match with minimum error shows the optimum location of the sound source and other parameters of interest.

Let us assume that sound signals propagate through Pekeris waveguide which has several parameters such as sound speed, density, and attenuation coefficient for both water and seabed (see Chapter 2). In real life applications, most of sea parameters are well-known [11]. For the sake of simplicity, we suppose that only seabed sound speed is un-known. Since source group delay of the received mode  $m$  is  $t_m(f) = t_s(f) + \frac{r}{v_m(f)}$  (equation 2-6), the distance between sound source/receiver ( $r$ ) effects the dispersion of the extracted mode. Therefore, two un-known parameters ( $r, c_b$ ) can be estimated through an iterative optimization algorithm [67]:

$$[\hat{r}, \hat{c}_b] = \arg \min \sum_{m \neq n} \sum_f ([t_m^{est}(f) - t_n^{est}(f)] - [t_m^{theo}(f, r, c_b) - t_n^{theo}(f, r, c_b)])^2 \quad (5-6)$$

where  $t_i^{est}$  and  $t_i^{theo}$  are the estimated and theoretical group delay of the  $i^{th}$  mode, respectively. The main reason for using group delays differences of modes  $m$  and  $n$  is to obviate the need to know the source time frequency law ( $t_s(f)$ ) which gives us information about how the source signal was modulated.

## 5.8 Depth Estimation

Like range estimation, an iterative approach is used for source depth estimation. Since amplitude of the received signal is proportional to the source depth (equation 2-2), amplitude of each mode is estimated from the received signal and it is compared with those obtained from the theoretical propagation model. To find the best matching between estimated and theoretical modes amplitudes, source depth parameter varies over a predefined range to generate different signal modes. The depth for which the similarity between estimated and theoretical amplitudes reaches maximum is considered as the estimated source depth.



The process of extracting modal components from the received signal is the same for range estimation [11]. First, warping transformation is applied on the received signal to attain warped signal, which is easier to extract modes from it. Then, TF filter is designed to extract the desired mode from the spectrogram of the warped signal. Finally, the inverse warping is performed to transform the filtered mode to the original domain.

After modes extraction, mean over frequency domain are computed, called mode excitation factors ( $C$ ). The mode excitation factors are then normalized:

$$C_m = \sum_m C_m(z_s)^2 = 1 \quad (5-7)$$

When the mode excitation factors are extracted and normalized, the comparison between  $m^{th}$  mode excitation factor obtained from theory ( $C_m^{theo}$ ) and the estimated one ( $C_m^{est}$ ) is made [69]:

$$\widehat{Z_s} = \arg \min \sum_m (C_m^{est}(Z_s) - C_m^{theo}(Z_s))^2 \quad (5-8)$$

It should be noted that unlike range estimation in which optimization is performed over different modes (equation 5-6), optimization is performed over the same modes in equation (5-8). This is due to the fact that after finding the optimum range through equation (5-6) and fixing it, modes do not change when source depth varies.

Figure 5.16 shows the overall flowchart of the acoustic localization technique based on modal filtering. Next section focuses on the experimental results.

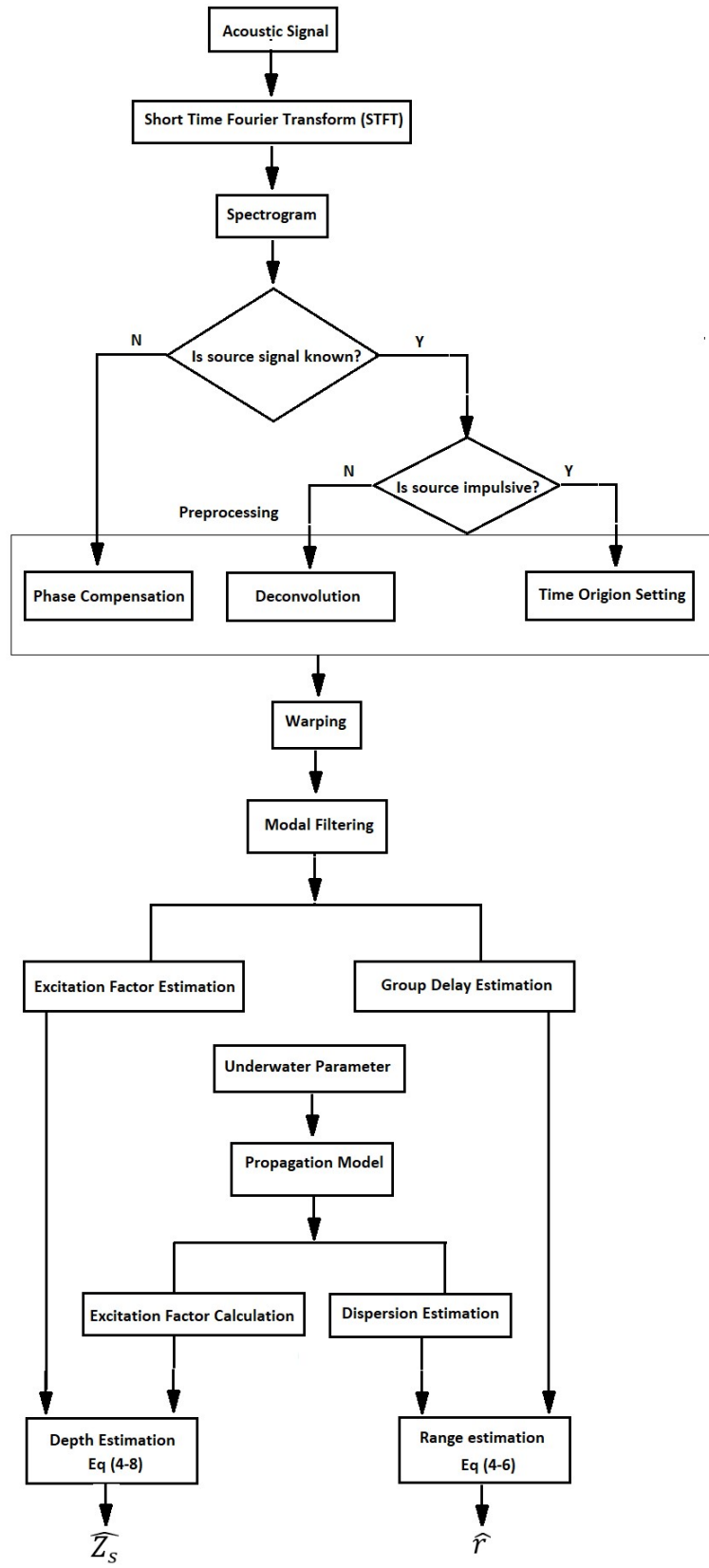


Figure 5.16: Overall flowchart of the proposed acoustic localization technique.

## **5.9 Summary:**

This chapter explained how warping can be applied more effectively on different signals. When some information about the source signal is available, warping can bring about more separable modes. Time origin setting, signal deconvolution, and phase compensation used for this purpose. Then, modal filtering was explained. Finally, range and depth of the source signal were estimated based on dispersion curves.

## CHAPTER 6

### Experimental Results

This section presents the evaluation results of the dispersion based acoustic underwater localization method. This method relies on an acoustic waveguide model to simulate sound propagation. In this thesis, we used Pekeris model which has been used frequently for shallow underwater applications. Different types of synthetic and real acoustic signals such as impulsive, non-impulsive signals with and without source signal knowledge will be used for the localization algorithm evaluation. We will also study the robustness of the localization method against various parameters like noise, waveguide factors, and warping function variables.

#### 6.1. Localization using synthetic data

Although different datasets are available for underwater acoustic processing [70] [71], they cannot be used for localization application, because range and depth information of the sound source are not provided. These datasets are mostly deployed for detection and classification of marine species (dolphin and mammal) and marine vehicles (ship and boat sounds).

To overcome this problem, this synthetic data sets, generated and propagated by an underwater waveguide, have been utilized [69][72]. We use the Pekeris model (see chapter 2) with the following parameters to create sound signals. Figure 6.1 shows the experimental configuration.

- (i) water column depth: 100 m;
- (ii) sound speed velocity in water: 1500 m/s;
- (iii) sound speed velocity in sediments: 1600 m/s;
- (iv) water density: 1000 kg/m<sup>3</sup>;
- (v) sediment density: 1500 kg/m<sup>3</sup>.

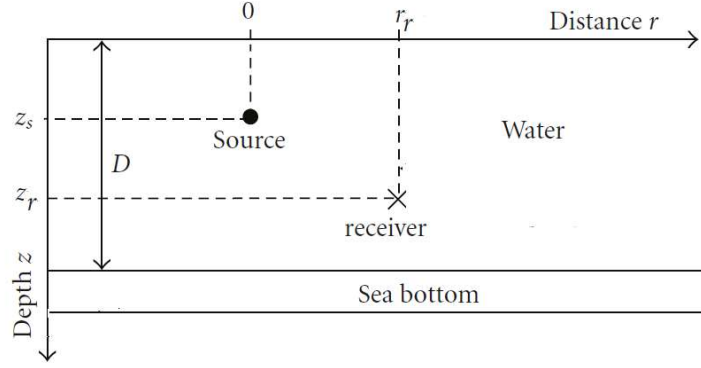


Figure 6.1: Experimental configuration.

The distance between source and receiver is 10 km. The received signal and its spectrogram are shown in figure.6.2 (a) and (b). It is obvious the received signal has 4 modes. Calculated and estimated dispersion curves are represented in figure.6.2 (c). Calculated dispersion curves (obtained from Pekeris model) are shown with circles, while estimated dispersion curves (obtained from the received signal) are shown with solid lines. As it can be seen, these curves are well-matched, so we expect an accurate range estimation. Figure.6.2 (d) shows the range estimation error, which is minimum at 9.4 km which is close to the true value (10 km).

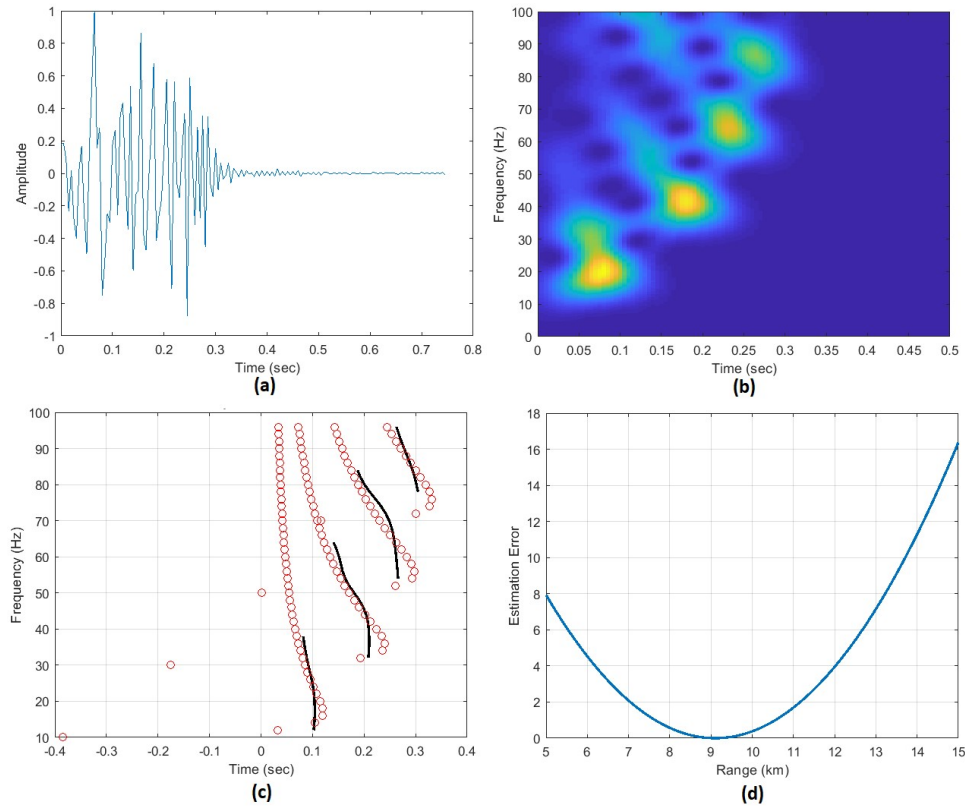


Figure 6.2: Sound signal localization.

- (a): The received signal in time domain. (b): Spectrogram of the received signal.  
(c): Calculated and estimated dispersion curves. (d): localization error.

### 6.1.1. Number of Modes Effect

Number and order of modes affect the localization accuracy, because the proposed method compares calculated and estimated dispersion curves over different modes (equation 5-6). Firstly, we explore the relationship between number of modes and range accuracy. According to Table.6.1, by increasing the number of modes, range estimation becomes more accurate. Secondly, importance of each mode is studied in Table.6.2. As it can be seen, the algorithm is not very sensitive to the mode couples.

Table 6.1: Results of range estimation for different number of modes.

Modes	Estimated Range (km)	Error (%)
1,2	9300	7
1,2,3	9500	5
1,2,3,4	9600	4

Table 6.2: Results of range estimation for mode couples.

Modes	Estimated Range (km)	Error (%)
1,2	9300	7
1,3	10600	6
1,4	10600	6
2,3	9500	5
2,4	10700	7
3,4	9300	7

### 6.1.2. Noise Effect

Underwater environment has various disturbances that affect traveling sound signal, called underwater acoustic noise. Such noises may have natural sources (such as rain and wind) or manmade sources (like shipping). Underwater acoustic noise is often modeled as white noise [73]. Figure 6.3 shows the effect of white noise on the modal separation and consequently on the range estimation accuracy.

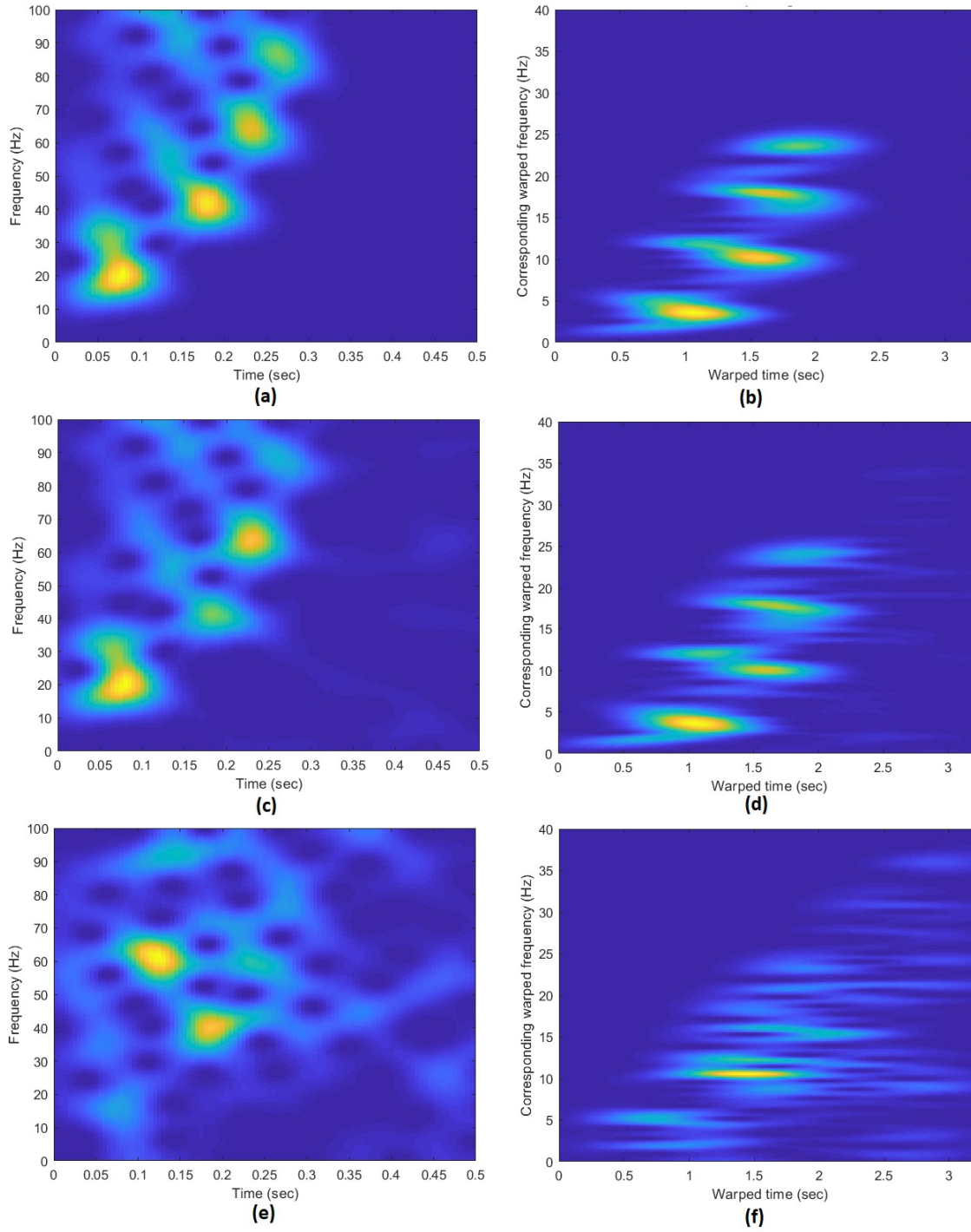


Figure 6.3: Noise effect on the modal separation.

- (a): Sound signal without noise in TF domain. (b): Warped signal in (a).  
(c): Contaminated signal with low noise (SNR=16 dB). (d): Warped signal of (c).  
(d): Contaminated signal with high noise (SNR=12 dB). (e): Warped signal of (d).

One can see that by reducing signal to noise ratio (SNR), modes distinction and separation become more challenging. For instance, when SNR is 12 dB, modes overlap each other, both in the original TF domain (figure 6.3 (e)) and warping domain (figure 6.3 (f)). Range estimation error as a function of noise strength is shown in figure 6.4. It is obvious that range estimation error declines sharply when SNR increases from 1 dB to 25 dB. This is due to the fact that noise is dominate in the signals with SNR less than 25 dB. When the signal is very good ( $25 \text{ dB} < \text{SNR} < 40 \text{ dB}$ ) or excellent ( $\text{SNR} > 40 \text{ dB}$ ), range error converges to 7%.

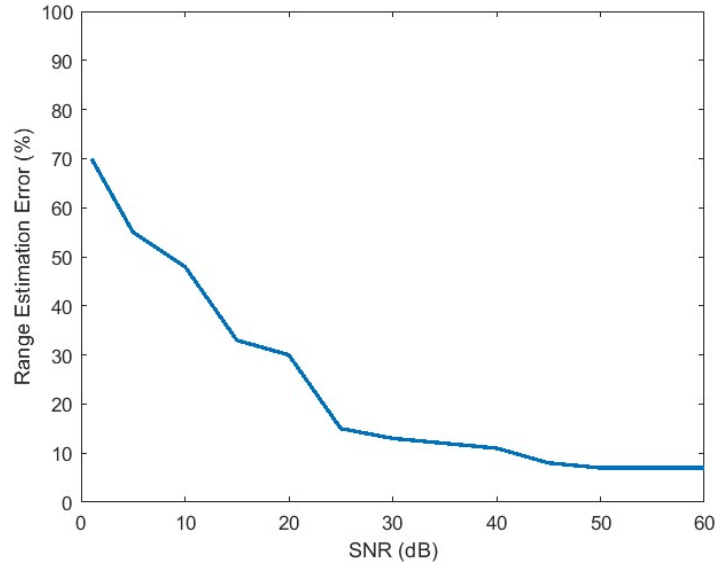


Figure 6.4: Noise effect on range estimation error.

### 6.1.3. Range Effect

The proposed acoustic localization method is based on dispersion phenomena which brings about separate modes. As it was explained in chapter 2, the longer the range, the more dispersion, and consequently the more separable modes. Therefore, in short ranges, modes are convoluted, and cannot be filtered properly. One can see in Figure.6.5 (a) that in short ranges (less than 1 km), the first three modes overlap, and the fourth mode is attenuated. This contributes to high error rate. When the distance between sound source and receiver is more than 5 km, modes are clearly distinguishable. Figure.6.6 indicates how range estimation accuracy precipitously declines at short ranges where dispersion is low.



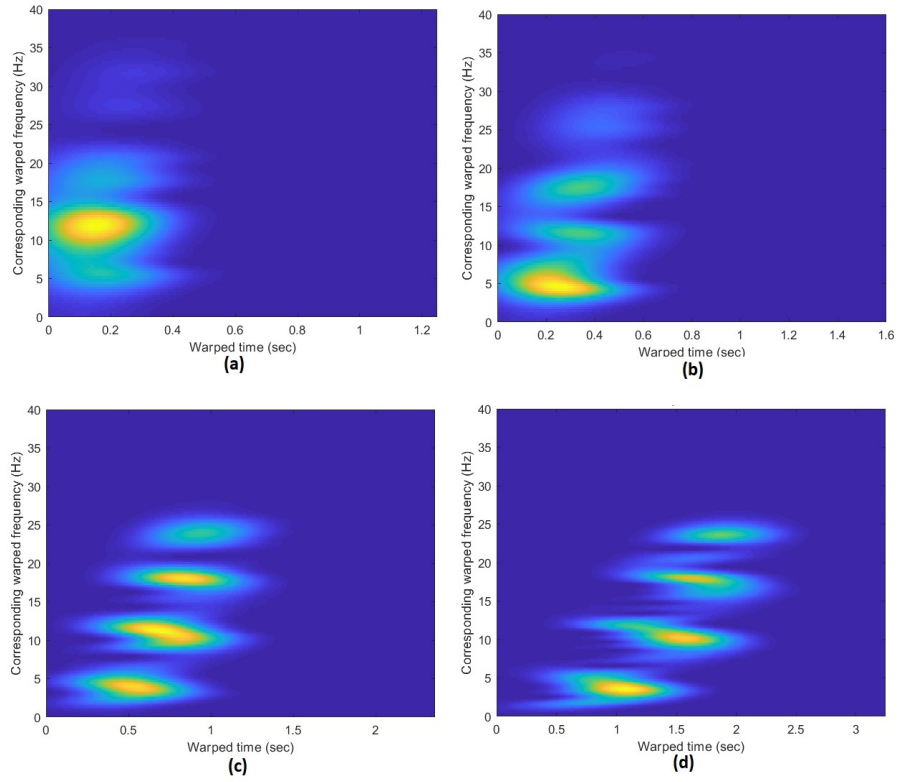


Figure 6.5: Effect of source/receiver distance on range estimation error.  
 (a): Received signal at 1 km range. (b): Received signal at 2 km range.  
 (c): Received signal at 5 km range. (d): Received signal at 10 km range.

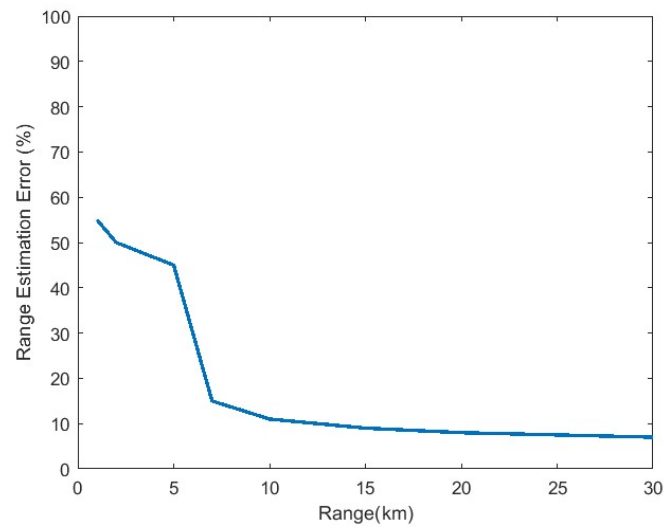


Figure 6.6: Range estimation error as a function of source/receiver distance.

#### 6.1.4. Waveguide Parameters Effect

As mentioned earlier in section.6.1, sound propagation depends on underwater waveguide parameters. We assumed that water sound speed ( $c_w$ ) and water depth ( $D$ ) are well-known, while seabed sound speed ( $c_b$ ) is unknown. Other parameters such as water and seabed densities ( $\rho_w, \rho_b$ ) are assumed to be known and fixed. In this section, sensitivity of the localization algorithm to the waveguide parameters is investigated. Experimental results show that range estimation is mainly influenced by the water sound speed, and other parameters do not affect the results. Figure.6.7. shows how range estimation error varies with the water sound speed variations. One can see that estimation error is minimum at  $c_w = 1550 \frac{m}{s}$  which is close to the true value of  $c_w = 1500 \frac{m}{s}$ . Experimental results show that range estimation is not sensitive to other waveguide parameters.

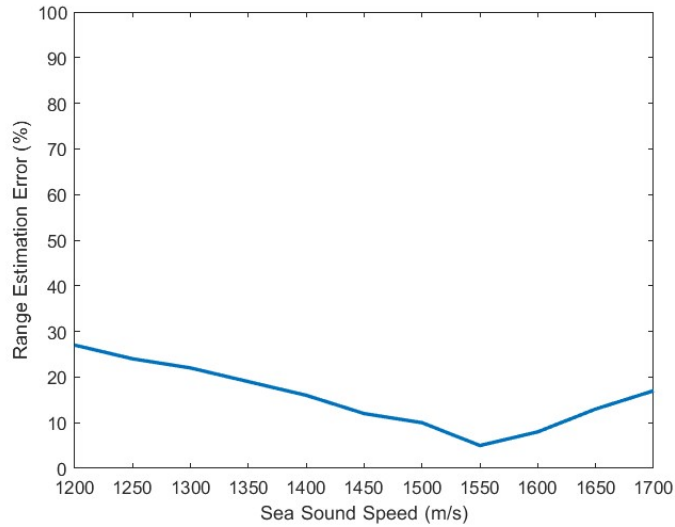


Figure 6.7: Range estimation error as a function of sea sound speed.  
True value of sea sound speed was 1500 m/s.

#### 6.1.5. Waveguide Model Effect

In the previous sections we used Pekeris waveguide to model sound propagation in a shallow water. In this section, other models will be used to explore the effect of waveguide models on the accuracy of the localization algorithm.

First, MATLAB Phased Array System Toolbox was employed to simulate a shallow water channel. This toolbox provides algorithms and applications for the design, simulation, and analysis of

sensor array systems in sonar applications. The sound source was modeled as an isotropic projector with `phased.IsotropicProjector` command. A multipath channel was created by `phased.IsoSpeedUnderwaterPaths` and `phased.MultipathChannel` to transmit the signal between the sound source and receiver. To have the same number of modes, 4 propagation paths was defined, including the direct path and reflections from the top and bottom surfaces. Because of the multiple propagation paths, the received signal is a superposition of multiple signals, which resembles the multi-modal signal in the Pekeris model. Table.6.3 compares the Pekeris and Multipath models performance. As it can be seen, the multipath model error is always more than the Pekeris model. This can be justified by the fact that in the multipath model, sea surface and seabed are highly reflective. In other words, sound propagation through seabed was neglected in this model.

Table 6.3: Compares between the Pekeris and Multipath models.

True Range value (km)	Estimated Range Value (km)	
	Pekeris	Multipath
8000	7520	7000
9000	8500	8050
10000	9600	9100
12000	11300	11040
15000	14100	13800
20000	18800	18600

## 6.2. Localization using real data

Performance of the localization algorithm was investigated by using synthetic sound signals in the previous section. This section aims to use real underwater sound signals to evaluate the localization algorithm. Three different groups of signals will be used for this purpose, an including impulsive signals, a signal with known waveform, and an unknown frequency modulated signal [67].

### 6.2.1. Impulsive Sound Localization

First, a gunshot sound that is an impulse signal is used for localization. Sound of some marine mammals such as North Pacific right whale can be regarded as an impulse signal. Figure.6.8 (a)

shows the signal in time domain, and its corresponding spectrogram is depicted in figure.6.8 (b). Four modes are completely visible in the spectrogram. One can also see ambient noise with frequency less than 20 Hz. As it was mentioned in Section.5.2, time origin selection step that determines the arrival of the fastest mode is important for impulsive sound warping. Figure.6.9 (a) shows the warped signal with wrong time origin selection ( $t=0.1$ s), resulting in bended modes in TF domain, which is difficult to be separated. After adjusting the time origin to  $t=0.3$ s, all modes are converted to horizontal lines in TF domain (Figure.6.9 (b)). We assume that water depth is 50m and water sound speed is 1450m/s. Figure.6.10 (a) shows that calculated and estimated dispersion curves are well-matched, expecting accurate localization estimation. As it can be seen from Figure.6.10 (b), localization error reaches the minimum at 9 km, which is close to true value (8.4 km).

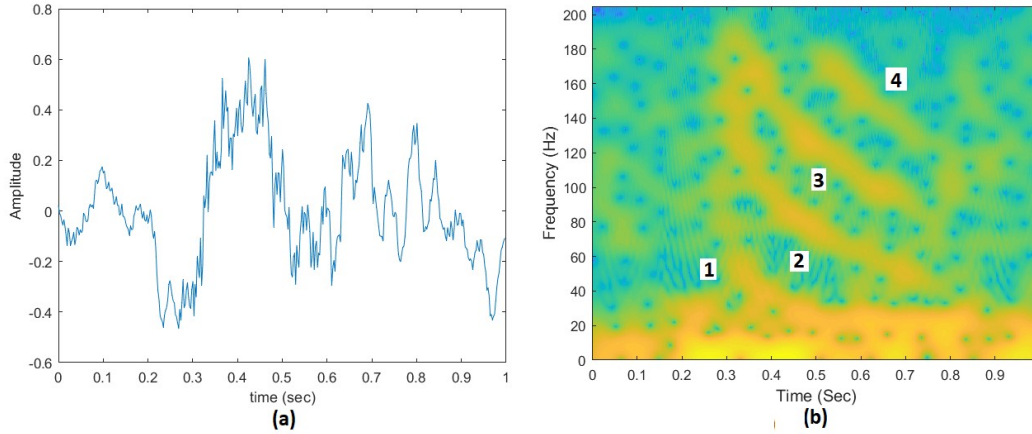


Figure 6.8: Impulsive signal in real world.  
(a): Time domain representation. (b): Spectrogram of the signal in (a).

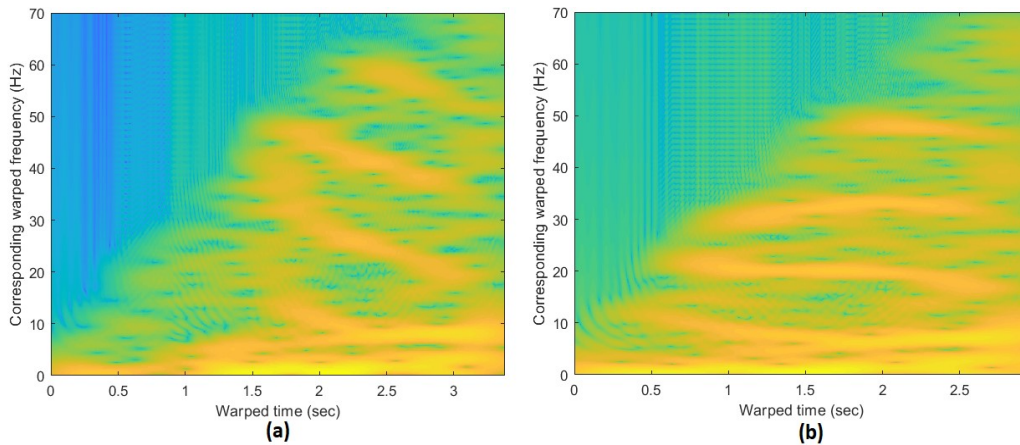


Figure 6.9: The effect of time origin selection on warped signal.  
(a): Wrong time origin selection. (b): Accurate time origin selection.

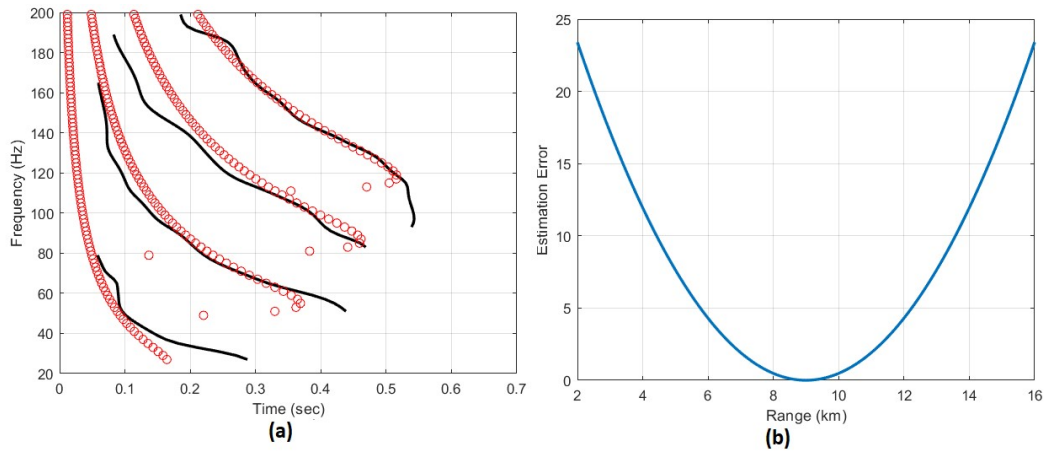


Figure 6.10: Localization result for real impulsive signal.  
(a): Calculated and estimated dispersion curves. (b): localization error.

### 6.2.2. Known Sound Localization

In this experience, a real underwater sound with known waveform is employed. The signal can be regarded as an impulsive signal ( $t=0.05s$ ), contaminated by several bubble pulses (figure.6.11 (a)). The received signal at  $r=4.8$  km is shown in figure.6.11 (b). Since we assumed that waveform for the source signal is known in advance, signal deconvolution is performed on the received signal (section.5.2). Figure.6.12 shows the effect of deconvolution on the warped signal. By comparing figure.6.12 (c) and figure.6.12 (d), one can see that after deconvolution and warping modes can be filtered more easily. In the next step, the effect of deconvolution is explored on the localization accuracy. According to figure.6.12 (a) calculated and estimated dispersion curves are not well-matched, resulting to inaccurate range estimation of  $r=3.3$  km which is not fully consistent with the true value  $r=4.8$  km. After deconvolution (figure.6.12 (b)), dispersion curves overlap, yielding to  $r=5.1$  km.

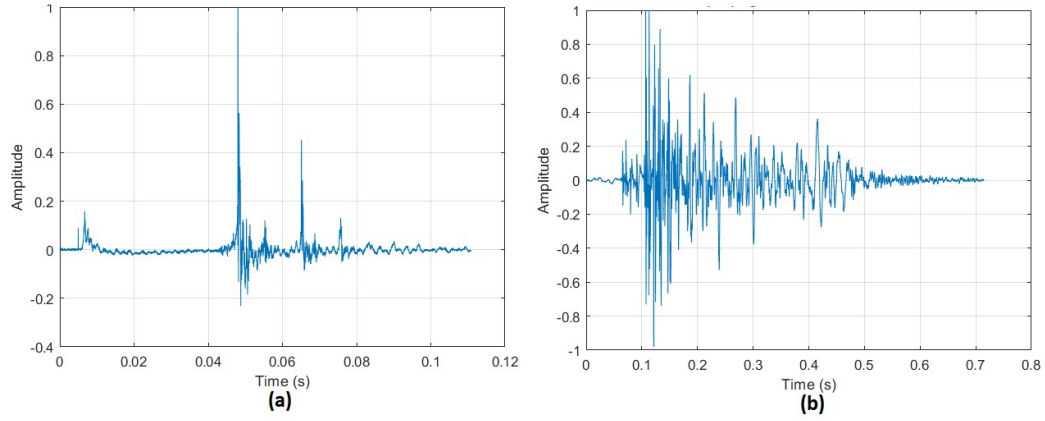


Figure 6.11: Real world signal in time domain.  
(a): Source signal. (b): Received signal.

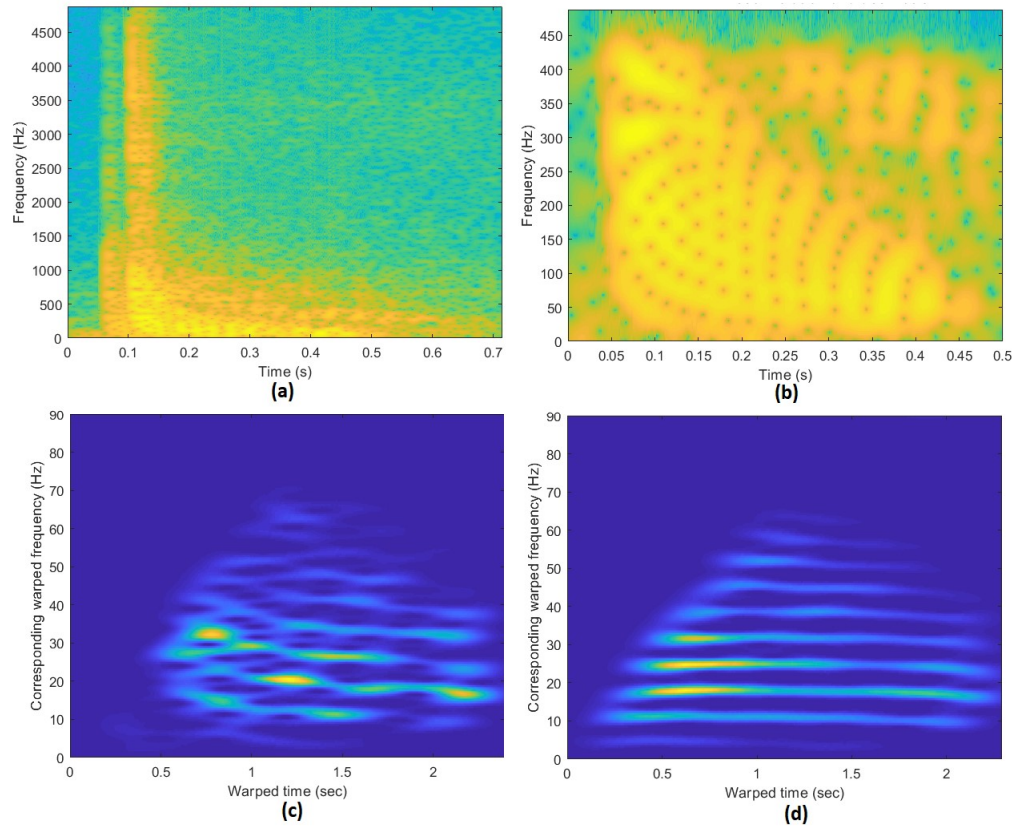


Figure 6.12: Received signal in TF domain.  
(a): Received signal without deconvolution. (b): Received signal with deconvolution.  
(c): Warped signal of (a). (d): Warped signal of (b).

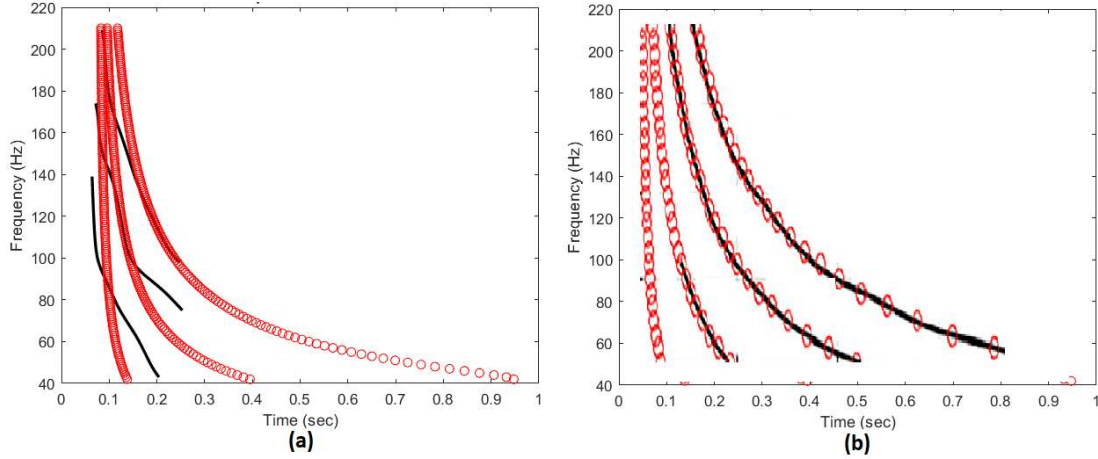


Figure 6.13: Calculated and estimated dispersion curves.  
(a): Dispersion curves without deconvolution. (b): Dispersion curves with deconvolution.

### 6.2.3. Unknown Sound Localization

As the last experiment, we aim to localize a bowhead whale based on its sound [67]. Figure.6.14 shows the received signal and its corresponding spectrogram. Three modes are utterly visible in the TF domain. Since waveform of emitted sounds of this type of species is unknown, phase compensation (section 5.3) is used instead of signal deconvolution. To do so, phase of the source signal is estimated from the first mode. Figure 6.15 (a) shows the manually selected TF law of the source used for phase compensation. After this preprocessing step, spectrogram of the signal looks like an impulse response (figure 6.15 (b)). The effect of phase compensation on the warped signal is also investigated in figure.6.15. One can see that first and second modes extensively overlap when phase compensation is not performed (figure 6.15 (c)). However, after phase compensation modes are completely separable (figure 6.15 (d)), resulting to better localization performance. Calculated and estimated dispersion curves are shown in figure.6.16 (a). These curves have mismatch which reduces the localization accuracy. According to figure.6.16 (b), range estimation error is minimum at 16.5 km that is close to  $14.1 \text{ km} \pm 1.8 \text{ km}$  recorded by other sensors. If phase compensation is not performed, localization estimation was 12.5 km.



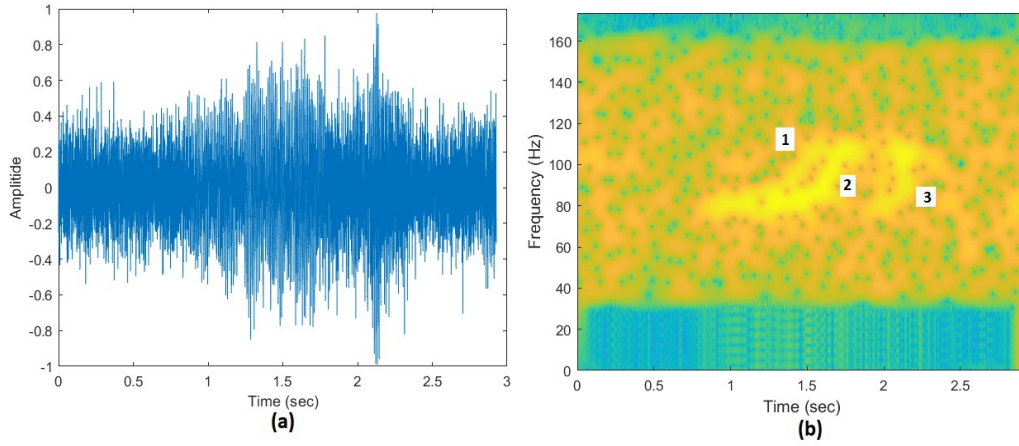


Figure 6.14: Dolphin sound signal.  
(a): Time domain representation. (b): Spectrogram of the signal in (a).

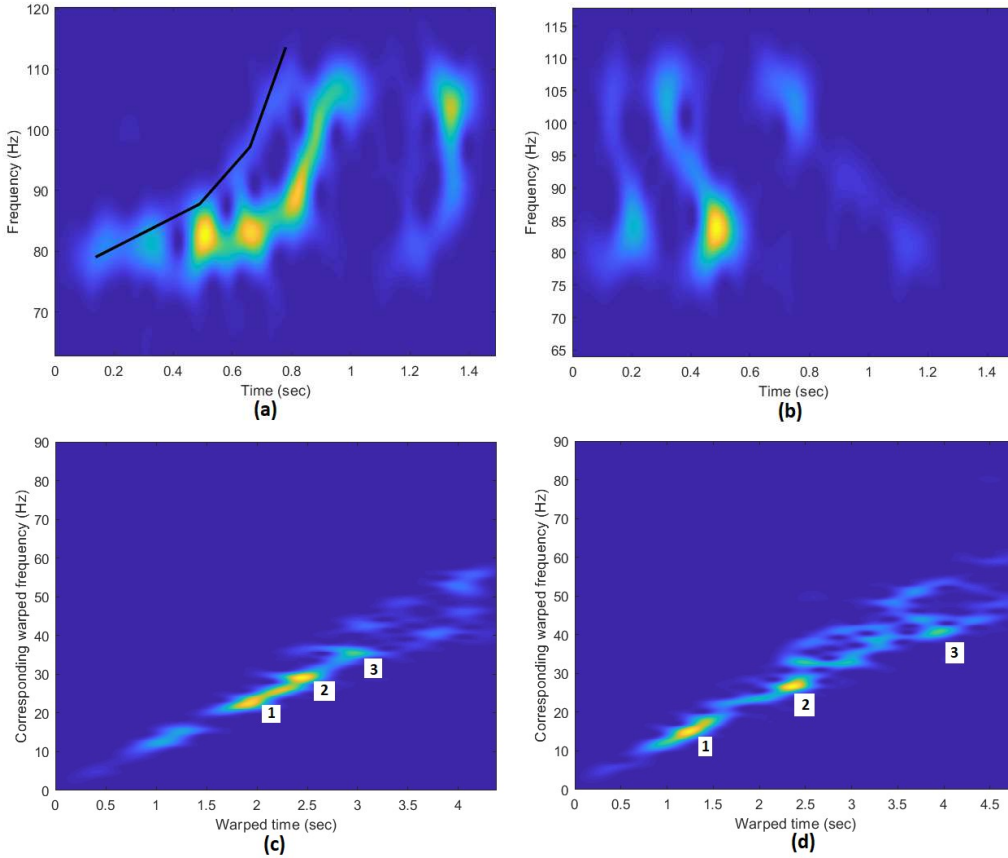


Figure 6.15: Effect of phase compensation on a real signal.  
(a): Estimated TF law of the source signal. (b): Spectrogram of the signal after phase compensation.  
(c): Warped signal without phase compensation. (d): Warped signal with phase compensation.



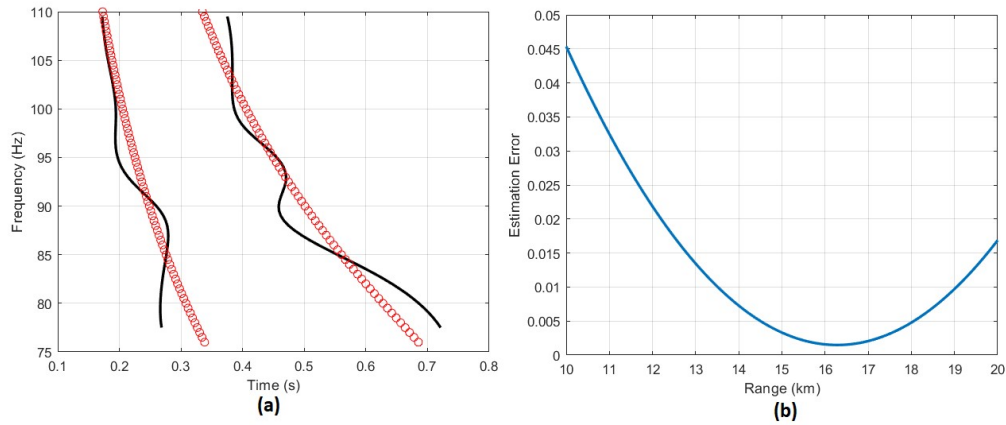


Figure 6.16: Localization result for a dolphin signal.  
 (a): Calculated and estimated dispersion curves. (b): localization error.

### 6.3. Summary:

This chapter presented experimental results. Both real and synthetic signals were utilized for acoustic sound localization. Effects of different parameters on the localization accuracy were explored.

## **CHAPTER 7**

### **Conclusion**

#### **7.1. Summary**

This thesis focused on sound source localization in shallow water. The proposed system was based modal dispersion mechanism, which is more visible in large ranges. Unlike conventional systems, only one hydrophone was adopted in this thesis. Warping technique was utilized to make arriving modes more distinguishable for modal filtering. After the modes were filtered manually, dispersion curves could be estimated more easily. To find the location of the sound source, the estimated dispersion curves were compared with calculated counterparts, obtained from the waveguide model. The range value with minimum error was regarded as the optimum estimation.

#### **7.2. Conclusion**

This thesis investigates the potential of acoustic signal processing methods for underwater source localization in shallow water. The experimental results show that warping technique can obviate the need for multiple-hydrophone systems, which are costly and difficult to set up. Although we used a simple, the Pekeris model, to study sound propagation, experimental results demonstrated that this model can accurately localize both synthetic and natural sounds in an isovelocity environment. These promising results can pave the way for utilizing other nonlinear signal processing techniques for source localization in other environments such as deep oceans or confined spaces. However, we found that lack of information about the propagation mechanism or sound source can lead to high errors.

#### **7.3. Future work**

The following functionalities can be added in the future:

- Performing localization in challenging environments. In this thesis we focused on shallow water environment in which sounds propagates with the same velocity in all directions. In deep water, however, sound speed varies with depth of water, causing modes to overlap more. Similarly, in a confined space with highly reflective boundaries, reflection of a slow-

moving mode may receive sooner than a fast mode. These situations bring about crossing modes in the TF domain, and warping technique fails to separate them. Other signal processing algorithms should be used to address these challenges.

- Localizing continuous signals. Relying on the modal separation, we only studied signals with limited time duration. Although most of natural sounds like marine mammals' sounds are transient, broadband signals produced by vehicles such as ships should also be considered. In these cases, fast mode of the succeeding signal may arrive sooner than the slow mode of the preceding signal. Prior know-how of the sound generator can mitigate this issue.
- Using multiple non-synchronized hydrophones. Synchronization of hydrophones in an array of sensors is not a trivial task. The received signal of each hydrophone can be warped individually to obviate the need for synchronization. Multiple non-synchronized hydrophone array may yield more accurate results.
- Testing with more natural sounds. In this work only a few real sound signals emitted by dolphins were used for localization. This is due to the fact that pinpointing the location of these species is tricky. In contrast, the true position of man-made signals can be obtained by global positioning system (GPS).

## REFERENCES/BIBLIOGRAPHY

### References

- [1]- M. Denny, *Blip, Ping & Buzz: Making Sense of Radar and Sonar* (The Johns Hopkins University Press, Baltimore, 2007).
- [2]- G. Le Touze, J. Torras, B. Nicolas and J. Mars, "Source localization on a single hydrophone," *OCEANS 2008*, Quebec City, QC, Canada, pp. 1-6, 2008.
- [3]- Julien Bonnel, Aaron M. Thode, Susanna B. Blackwell, Katherine Kim, and A. Michael Macrander," Range estimation of bowhead whale (*Balaena mysticetus*) calls in the Arctic using a single hydrophone", *The Journal of the Acoustical Society of America* 136, 145, 2014.
- [4]- Seunghyun Yoon, Haesang Yang, and Woojae Seong," Deep learning-based high-frequency source depth estimation using a single sensor", *The Journal of the Acoustical Society of America* 149, 1454, 2021.
- [5]- Douglas A. Abraham, "Underwater acoustic signal processing modeling, detection, and estimation", Springer, 2019.
- [6]- H. Shen, Z. Ding, S. Dasgupta, and C. Zhao, "Multiple source localization in wireless sensor networks based on time of arrival measurement," *IEEE Transactions on Signal Processing*, vol. 62, no. 8, pp. 1938–1949, 2014.
- [7]- Z. Wang, J.-A. Luo, and X.-P. Zhang, "A novel location penalized maximum likelihood estimator for bearing-only target localization," *IEEE Transactions on Signal Processing*, vol. 60, no. 12, pp. 6166–6181, 2012.
- [8]- Jensen, F., Kuperman, W., Porter, M., and Schmidt, H. , "Computational Ocean Acoustics", 2nd ed. American Institute of Physics, New York, 2011.
- [9]- González-García, J.; Gómez-Espinosa, A.; Cuan-Urquizo, E.; García-Valdovinos, L.G.; Salgado-Jiménez, T.; Cabello, J.A.E. "Autonomous Underwater Vehicles: Localization, Navigation, and Communication for Collaborative Missions", *Appl. Sci.* 10, 1256, 2020.
- [10]- Shaukat, N.; Ali, A.; Javed Iqbal, M.; Moinuddin, M.; Otero, P. "Multi-Sensor Fusion for Underwater Vehicle Localization by Augmentation of RBF Neural Network and Error-State Kalman Filter", *Sensors* 21, 1149, 2021.
- [11]- Julien Bonne, Salvatore Caporale, Aaron Thode, "Waveguide mode amplitude estimation using warping and phase compensation", *The Journal of the Acoustical Society of America* 141, 2243, 2017.
- [12]- P. J. B. Sánchez, M. Papaelias and F. P. G. Márquez, "Autonomous underwater vehicles: Instrumentation and measurements," in *IEEE Instrumentation & Measurement Magazine*, vol. 23, no. 2, pp. 105-114, 2020.

- [13]- Peng Wu, Shaojing Su, Zhen Zuo, Xiaojun Guo, Bei Sun, and Xudong Wen,” Time Difference of Arrival (TDoA) Localization Combining Weighted Least Squares and Firefly Algorithm”, *Sensors* (Basel). 19(11): 2554, 2019.
- [14]- Liam Paull, Sajad Saeedi, Mae Seto, and Howard Li,” AUV Navigation and Localization: A Review”, *IEEE JOURNAL OF OCEANIC ENGINEERING*, VOL. 39, NO. 1, pp. 131-149, 2014.
- [15]- M. W. Khan, Y. Zhou, and G. Xu,” Modeling of acoustic propagation channel in underwater wireless sensor networks”, *International Conference on Systems and Informatics (ICSAI 2014)*, pp. 586–590, 2014.
- [16]- A.-M. Ahmad, J. Kassem, M. Barbeau, E. Kranakis, S. Porretta and J. Garcia-Alfaro,” Doppler Effect in the Acoustic Ultra Low Frequency Band for Wireless Underwater Networks”, *Mobile Networks and Applications*, volume 23, pp. 1282–1292, 2018.
- [17]- Frederic Sturm, Julien Bonnel,” Time-frequency analysis of broadband sound pulse propagation in 3-D oceanic waveguides”, *11th European Conference on Underwater Acoustics*, 2012.
- [18]- Michael G. Brown, “Time-warping in underwater acoustic waveguides”, *The Journal of the Acoustical Society of America* 147, 898, 2020.
- [19]- Afonso Mateus Bonito,” Acoustic system for ground truth underwater positioning in DEEC’s test tank”, *University Do Porto*, Master Thesis, 2019.
- [20]- Ashfaq Ahmed Bhatti; Sartaj Khan; Huang Yiwang,” Numerical Simulation of Shallow Water Propagation using Normal Mode Theory”, *International Bhurban Conference on Applied Sciences & Technology*, pp. 1-5, 2019.
- [21]- Qian, Z.; Shang, D.; Hu, Y.; Xu, X.; Zhao, H.; Zhai, J. A Green’s Function for Acoustic Problems in Pekeris Waveguide Using a Rigorous Image Source Method. *Appl. Sci.*, 11, 2722, 2021.
- [22]- G. N. Kuznetsov, A. N. Stepanov, “Approximate analytic representations of laws of attenuation in vector-scalar fields of multipole sources in a Pekeris waveguide”, *Acoustical Physics* volume 63, pages 660–672, 2017.
- [23]- Jensen, F., Kuperman, W., Porter, M., and Schmidt, H., “Computational Ocean Acoustics”, 2nd ed. ,*American Institute of Physics*, New York, 2011.
- [24]- ALUKO,O., “Implementation and Application of dispersion-based waveguide models for shallow-water sonar processing”, *Illinois Institute of Technology*, Master Thesis, 2002.
- [25]- D. Iatsenko, “Nonlinear Mode Decomposition”, *Springer*, 2015.
- [26]- J. Nathan Kutz , Steven L. Brunton , Bingni W. Brunton and Joshua L. Proctor,” Dynamic Mode Decomposition: Data-Driven Modeling of Complex Systems”, *Society of Industrial and Applied Mathematics*, 2016.

- [27]- M. H. Tanveer, H. Zhu, W. Ahmed, A. Thomas, B. M. Imran and M. Salman, "Mel-spectrogram and Deep CNN Based Representation Learning from Bio-Sonar Implementation on UAVs," 2021 International Conference on Computer, Control and Robotics (ICCCR), pp. 220-224, 2021.
- [28]- E. Mogi and T. Ohtsuki, "Heartbeat detection with Doppler radar based on spectrogram," 2017 IEEE International Conference on Communications (ICC), pp. 1-6, 2017.
- [29]- Abdellah Kacha, Francis Grenez, Juan Rafael Orozco-Arroyave, Jean Schoentgen, "Principal component analysis of the spectrogram of the speech signal: Interpretation and application to dysarthric speech", *Computer Speech & Language*, Volume 59, Pages 114-122, 2020.
- [30]- M. W. Khan, Y. Zhou, and G. Xu," Modeling of acoustic propagation channel in underwater wireless sensor networks", *International Conference on Systems and Informatics (ICSAI 2014)*, pp. 586–590, 2014.
- [31]- Michael J. Bianco, Peter Gerstoft, James Traer, Emma Ozanich, Marie A. Roch, Sharon Gannot, and Charles-Alban Deledalle," Machine learning in acoustics: Theory and applications", *The Journal of the Acoustical Society of America* 146, 3590, pp. 3590–3628, 2019.
- [32]- Z. Gong, C. Li and F. Jiang, "A Machine Learning-Based Approach for Auto-Detection and Localization of Targets in Underwater Acoustic Array Networks," in *IEEE Transactions on Vehicular Technology*, vol. 69, no. 12, pp. 15857-15866, 2020.
- [33]- J. Yan, Y. Gong, C. Chen, X. Luo and X. Guan, "AUV-Aided Localization for Internet of Underwater Things: A Reinforcement-Learning-Based Method," in *IEEE Internet of Things Journal*, vol. 7, no. 10, pp. 9728-9746, 2020.
- [34]- Haiqiang Niu, Emma Reeves, and Peter Gerstoft," Source localization in an ocean waveguide using supervised machine learning", *The Journal of the Acoustical Society of America* 142, 1176, 2017.
- [35]- Amir Horri, "Underwater Localization in a Confined Space Using Acoustic Positioning and Machine Learning", Master thesis, University of Windsor, 2021.
- [36]- X. You, Z. Lv, Y. Ding, W. Su and L. Xiao, "Reinforcement Learning Based Energy Efficient Underwater Localization," *International Conference on Wireless Communications and Signal Processing (WCSP)*, pp. 927-932, 2020.
- [37]- A. Testolin and R. Diamant, "Underwater Acoustic Detection and Localization with a Convolutional Denoising Autoencoder," *8th International Workshop on Computational Advances in Multi-Sensor Adaptive Processing (CAMSAP)*, pp. 281-285, 2019.
- [38]- Y. Dong, Z. Li, R. Wang and K. Zhang, "Poster Abstract: Range-Based Localization in Underwater Wireless Sensor Networks Using Deep Neural Network," *16th ACM/IEEE International Conference on Information Processing in Sensor Networks (IPSN)*, pp. 321-322, 2017.
- [39]- Riwal Lefort, Gaultier Real, Angélique Drémeau," Direct regressions for underwater acoustic source localization in fluctuating oceans", *Applied Acoustics*, 116, pp. 303–310, 2017.

- [40]- Yun Wang, and Hua Peng,” Underwater acoustic source localization using generalized regression neural network”, *The Journal of the Acoustical Society of America* 143, 2321, pp. 2321–2331, 2018.
- [41]- L. Perotin, A. Défossez, E. Vincent, R. Serizel and A. Guérin, "Regression Versus Classification for Neural Network Based Audio Source Localization," 2019 IEEE Workshop on Applications of Signal Processing to Audio and Acoustics (WASPAA), pp. 343-347, 2019.
- [42]- F. Grijalva, J. Larco and P. Mejía, "A Virtual Listener For HRTF-Based Sound Source Localization Using Support Vector Regression," 2018 IEEE Third Ecuador Technical Chapters Meeting (ETCM), pp. 1-5, 2018.
- [43]- A. Brendel and W. Kellermann, "Distributed Source Localization in Acoustic Sensor Networks Using the Coherent-to-Diffuse Power Ratio," *IEEE Journal of Selected Topics in Signal Processing*, vol. 13, no. 1, pp. 61-75, 2019.
- [44]- Y Lee, J Choi, NY Ko, HT Choi,” Probability-based recognition framework for underwater landmarks using sonar images”, *Sensors*, 17(9), 1953, 2017.
- [45]- G Han, S Li, C Zhu, J Jiang, W Zhang,” Probabilistic Neighborhood-Based Data Collection Algorithms for 3D Underwater Acoustic Sensor Networks“, *Sensors*, 17(2), 316, 2017.
- [46]- G. Han, H. Wang, S. Li, J. Jiang and W. Zhang, "Probabilistic Neighborhood Location-Point Covering Set-Based Data Collection Algorithm With Obstacle Avoidance for Three-Dimensional Underwater Acoustic Sensor Networks," *IEEE Access*, vol. 5, pp. 24785-24796, 2017.
- [47]- J. Choi and H. Choi, "Multi-target localization of underwater acoustic sources based on probabilistic estimation of direction angle," *OCEANS*, pp. 1-6, 2015.
- [48]- K.-C. Lee, J.-S. Ou, and M.-C. Huang, “Underwater acoustic localization by principal components analyses based probabilistic approach,” *Appl. Acoust.* 70(9), pp. 1168–1174, 2009.
- [49]- Edmund J. Sullivan,” *Model-Based Processing for Underwater Acoustic Arrays*”, Springer, 2015.
- [50]- Xinya Li, Zhiqun Daniel Deng, Lynn T. Rauchenstein, and Thomas J. Carlson,” Contributed Review: Source-localization algorithms and applications using time of arrival and time difference of arrival measurements”, *Review of Scientific Instruments*, 87, 041502, 2016.
- [51]- Afonso Mateus Bonito,” *Acoustic system for ground truth underwater positioning in DEEC’s test tank*”, University Do Porto, Master Thesis, 2019.
- [52]- João Miguel Fernandes Magalhães,” *Improving Time of Arrival Estimation Using Compensated Acoustic Signals*”, University Do Porto, Master Thesis, 2018.
- [53]- Peng Wu, Shaojing Su, Zhen Zuo, Xiaojun Guo, Bei Sun, and Xudong Wen,” Time Difference of Arrival (TDoA) Localization Combining Weighted Least Squares and Firefly Algorithm”, *Sensors (Basel)*. 19(11): 2554, 2019.

- [54]- F. Liu, H. Chen, L. Zhang and L. Xie, "Time-Difference-of-Arrival-Based Localization Methods of Underwater Mobile Nodes Using Multiple Surface Beacons," *IEEE Access*, vol. 9, pp. 31712-31725, 2021.
- [55]- L. Zhang, T. Zhang, H. -S. Shin and X. Xu, "Efficient Underwater Acoustical Localization Method Based On Time Difference and Bearing Measurements," *IEEE Transactions on Instrumentation and Measurement*, vol. 70, pp. 1-16, 2021.
- [56]- Saleheh Poursheikhali and Hossein Zamiri-Jafarian," Received signal strength based localization in inhomogeneous underwater medium", *Signal Processing*, Volume 154, Pages 45-56, 2019.
- [57]- Saleheh Poursheikhali and Hossein Zamiri-Jafarian," Source localization in inhomogeneous underwater medium using sensor arrays: Received signal strength approach", *Signal Processing*, Volume 183, 108047, 2021.
- [58]- Kay L. Gemba, William S. Hodgkiss, and Peter Gerstoft," Adaptive and compressive matched field processing", *The Journal of the Acoustical Society of America* 141, 92, 2017.
- [59]- AG Sazontov, AI Malekhanov," Matched field signal processing in underwater sound channels", *Acoustical Physics*, volume 61, pages 213–230, 2015.
- [60]- D. Tollefsen and S. E. Dosso, "Source Localization with Multiple Hydrophone Arrays via Matched-Field Processing," *IEEE Journal of Oceanic Engineering*, vol. 42, no. 3, pp. 654-662, 2017.
- [61]- R. Vivek and P. Vadakkepat, "Multiple signal classification (MUSIC) based underwater acoustic localization module (UALM) for AUV," *IEEE Underwater Technology (UT)*, pp. 1-4, 2015.
- [62]- L. Zhang, J. Huang, Q. Zhang, and Y. Hou, "Normal-mode based music for bearing estimation in shallow water," in *Proceedings of the 5th IEEE Sensor Array and Multichannel Signal Processing Workshop*, pp. 91–94, 2008.
- [63]- Veerendra Dakulagi," Robust Modified Multiple Signal Classification Algorithm for Direction of Arrival Estimation", *Wireless Personal Communications*, volume 115, pages 2535–2550, 2020.
- [64]- Ammari, H.; Iakovleva, E.; Lesselier, D," A MUSIC algorithm for locating small inclusions buried in a half-space from the scattering amplitude at a fixed frequency". *Multiscale Model. Simul.* 3, 597–628, 2005.
- [65]- W Shang, W Xue, Y Li, X Wu, Y Xu," An Improved Underwater Electric Field-Based Target Localization Combining Subspace Scanning Algorithm and Meta-EP PSO Algorithm", *J. Mar. Sci. Eng.*, 8(4), 232, 2020.
- [66]- Alan V. Oppenheim, "Discrete-Time Signal Processing", Pearson Education, 1999.
- [67]- Julien Bonnel, Aaron Thode, Dana Wright, and Ross Chapman, "Nonlinear time-warping made simple: A step-by-step tutorial on underwater acoustic modal separation with a single hydrophone", *The Journal of the Acoustical Society of America* 147, 1897, 2020.



- [68]- François Auger, Patrick Flandrin, Olivier Lemoine, “Time-Frequency Toolbox Reference Guide”, 2005.
- [69]- Lopatka, M., Le Touzé, G., Nicolas, B. et al. Underwater Broadband Source Localization Based on Modal Filtering and Features Extraction. EURASIP J. Adv. Signal Process. 304103, 2010.
- [70]- Hristo Zhivomirov, Ivaylo Nedelchev, Georgi Dimitrov, “Dolphins Underwater Sounds Dataset”, IEEE DataPort, 2020.
- [71]- David Santos-Domínguez, Soledad Torres-Guijarro, Antonio Cardenal-López, Antonio Pena-Gimenez, “ShipsEar: An underwater vessel noise database”, Applied Acoustics, Volume 113, Pages 64-69, 2016.
- [72]- Maciej Lopatka, Barbara Nicolas, Grégoire Le Touzé, Xavier Cristol, Bruno Chalindar, Jerome Mars, Dominique Fattaccioli, “Robust Underwater localization for Ultra Low frequency sources in operational context”, 3rd International Conference & Exhibition on Underwater Acoustic Measurements: Technologies & Results, 2009.
- [73]- A. Z. Sha'ameri, Y. Y. Al-Aboosi and N. H. H. Khamis, "Underwater Acoustic Noise Characteristics of Shallow Water in Tropical Seas," International Conference on Computer and Communication Engineering, pp. 80-83, 2014.

## **VITA AUCTORIS**

Luca Saeid was born in 1990 in Tehran, Iran. he graduated from Dubai International High School in Dubai, U.A.E in 2009. From there he went on to the St. Clair College where he obtained a three year Diploma in International Business in 2014. He then went on to the University of Windsor where he obtained a BA.Sc in Mechanical Engineering in 2018. He is currently a candidate for the Masters of Applied Science in Electrical and Computer Engineering at the University of Windsor and hopes to graduate in Summer 2021.